Grain Boundary Properties and Their Impact on Texture Development

A.D. Rollett, D. Saylor, J. Gruber,
G.S. Rohrer, M. Taheri, D.J. Srolovitz,
C.-S. Kim , T. Sano, T. Bennett

Carnegie Mellon University,
Pittsburgh, PA, USA

Penn State
Nov. 2004

With thanks to
P. Manohar, M. Alvi, A. Brahme, M. Upmanyu, G. Gottstein, L. Shvindlerman, D. Molodov, B.L. Adams, R. Larsen…

Carnegie Mellon MRSEC

Support from NSF-DMR, DOE-BES, PTIA, Alcoa, DoD/HPCMO

Outline

- Motivation for studying grain boundaries: many boundary properties (hence, material properties) depend on all 5 parameters
- *Coincident Site Lattice (CSL)* theory not consistent with facts: *average surface energy* is more useful
- Grain boundary mobility: 38°<111> *is* the high mobility boundary type (sometimes!)
- Integration of properties and evolution: anisotropic properties produces variations in boundary populations and/or texture
- Overview of grain boundary properties

Are polycrystals just soap froths? No!

- Measured dihedral angles are far from the 120° found in froths
- Grain boundary is sensitive to the boundary normal as well as (crystal) misorientation
- Theory shows that g.b. energy is expected to be correlated with surface energies
- Simulation of grain growth indicates a strong correlation between g.b. energy and population
- Texture development can occur during grain growth - linked to non-random initial textures, both mobility and energy anisotropy play a role

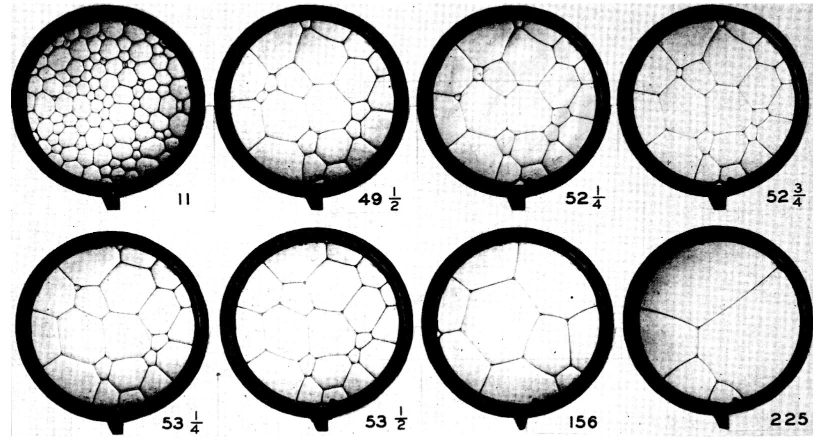

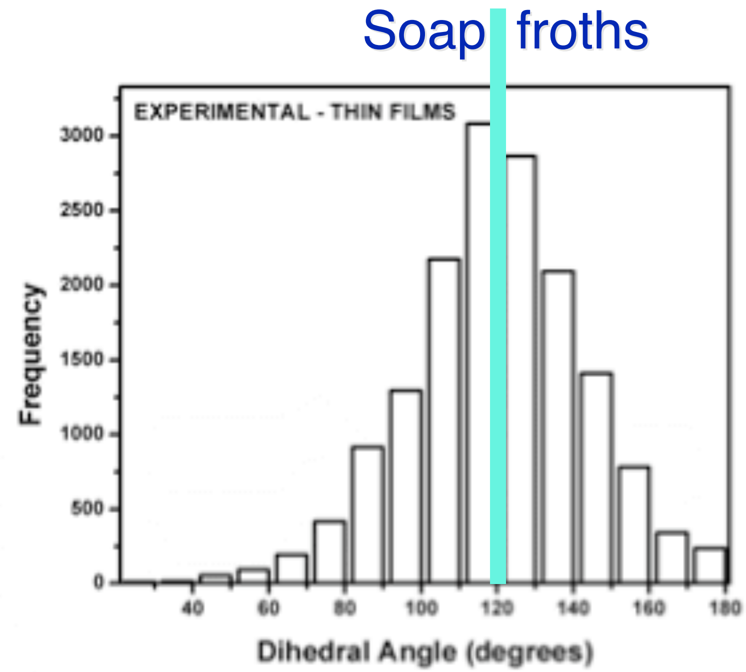

Grain Boundary Sliding

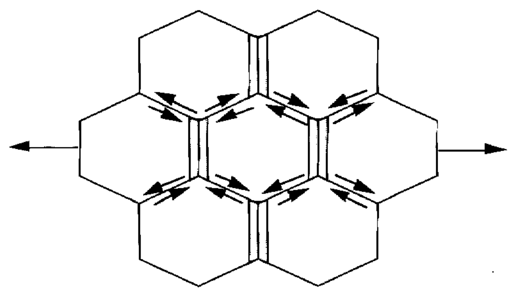

Figure 7.9 An array of grains showing the coupling between grain boundary sliding and diffusional elongation. (Adapted from Cook and Pharr, 1994, reproduced courtesy of VCH Publishers, Weinheim, Germany.)

- Grain boundary sliding should be very structure dependent. No surprise therefore that Biscondi's results show that the rate at which boundaries slide is highly dependent on misorientation; in fact there is a threshold effect with no sliding below a certain misorientation at a given temperature.

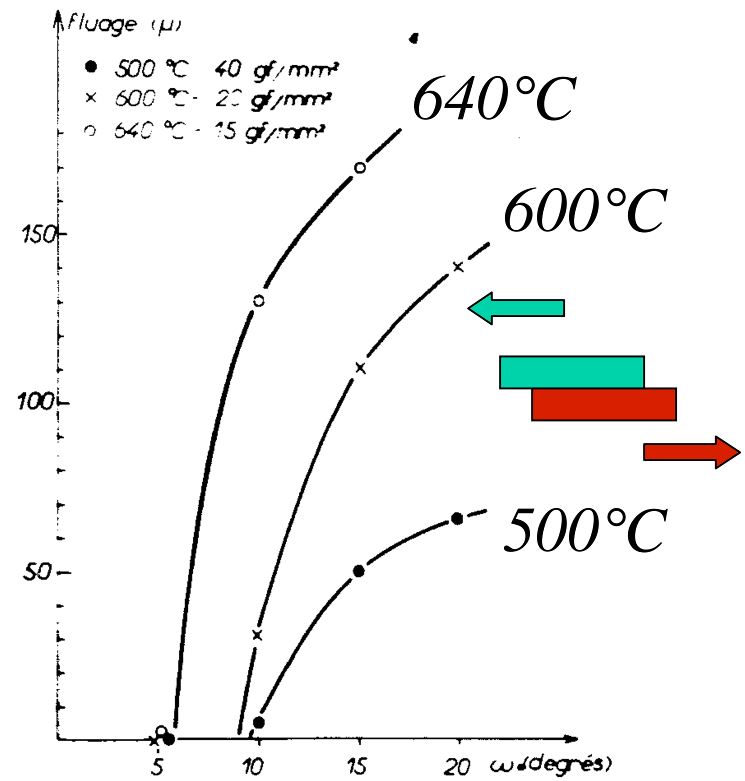

Fig. 23. — *Fluages mesurés au bout de* 100 mn, *dans diverses conditions de température et de charge, pour des joints de faible désorientation.*

Biscondi, M. and C. Goux (1968). "Fluage intergranulaire de bicristaux orientés d'aluminium." Mémoires Scientifiques Revue de Métallurgie **55**(2): 167-179.

Earing-Texture Correlation

deformation texture ⇒ 45° ears

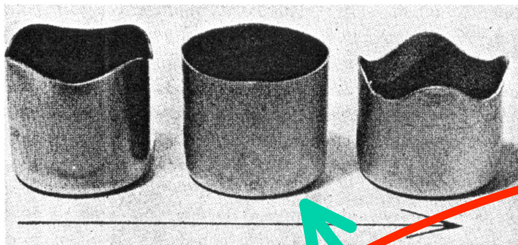

Figure 14-10 Earing behavior of cups made from three different copper sheets. Arrow indicates rolling direction of the sheets. From D. V. Wilson and R. D. Butler, *J. Inst. Met.*, 90 (1961–2), pp. 473–83.

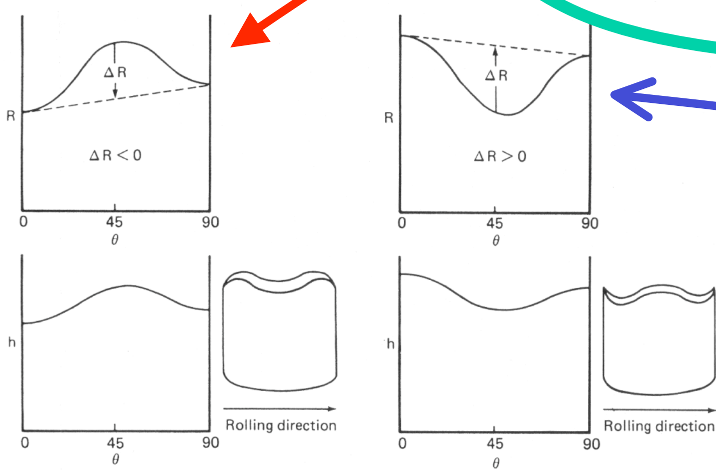

Figure 14-11 Relation of earing to angular variations of R. Here, h is the wall height.

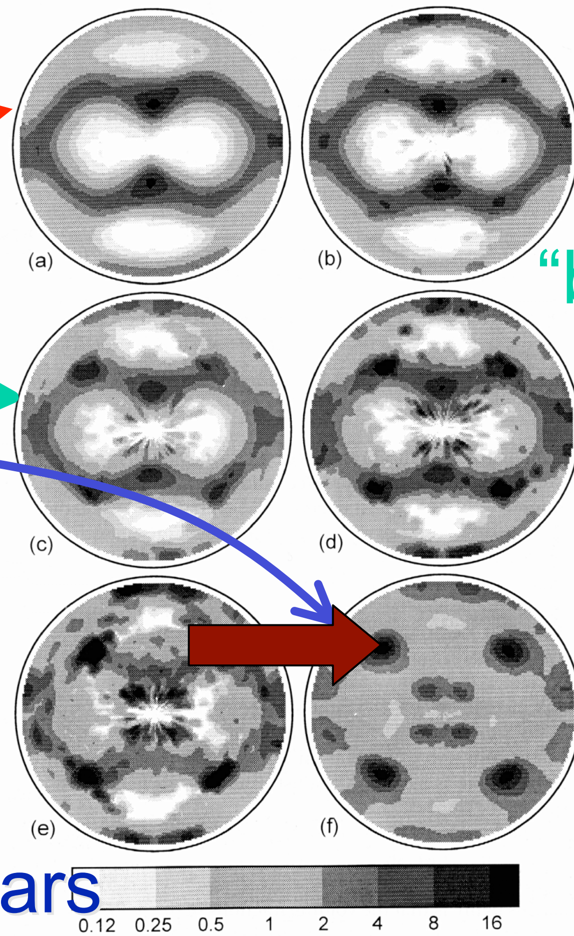

"balanced" texture

annealing texture ⇒ 0,90° ears

Other applications: capacitor foils; HTSC substrates

Grain Boundary Diffusion

- Especially for high symmetry boundaries, there is a very strong anisotropy of diffusion coefficients as a function of boundary type. This example is for Zn diffusing in a series of <110> symmetric tilts in copper.

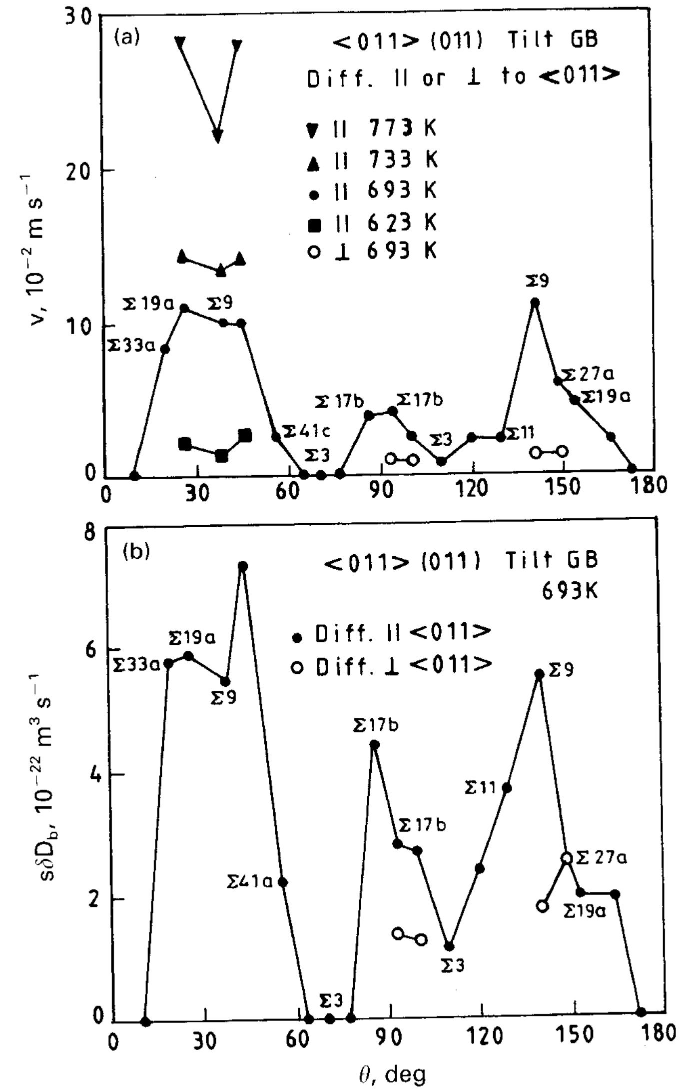

38 Kinetics of diffusion induced grain boundary migration in Cu bicrystals exposed to Zn vapour in terms of *a* variation of boundary velocity *v*, and *b* grain boundary chemical diffusion triple product $s\delta D_b$, as function of boundary misorientation angle θ for diffusion parallel (∥) and perpendicular (⊥) to ⟨011⟩ tilt axis of symmetric grain boundaries (GBs) with specific Σ values (*see* Ref. 100)

Complexity in Grain Boundary Studies

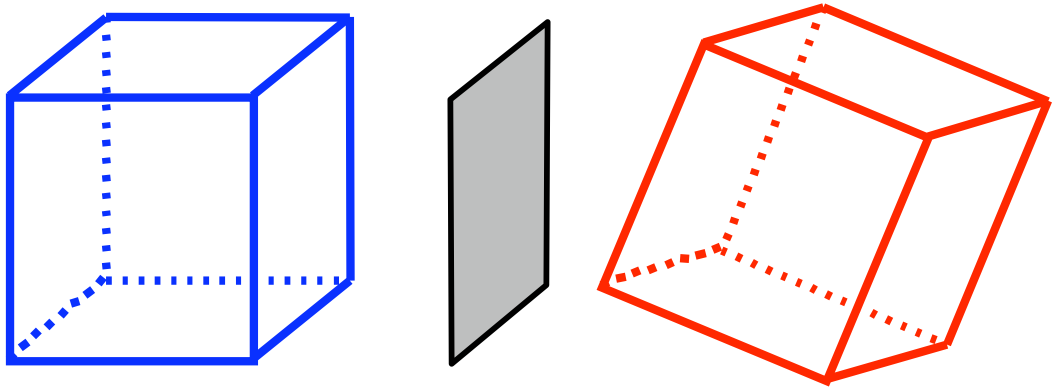

Lattice Misorientation, Δg (3)

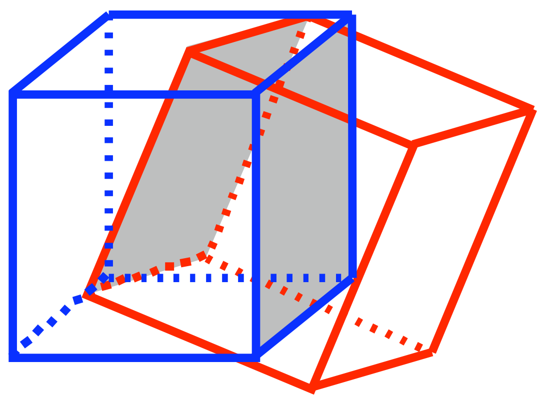

Boundary Plane, **n** (2)

Grain Boundaries have 5 Macroscopic Degrees of Freedom

Advantage of the Mesoscale Approach

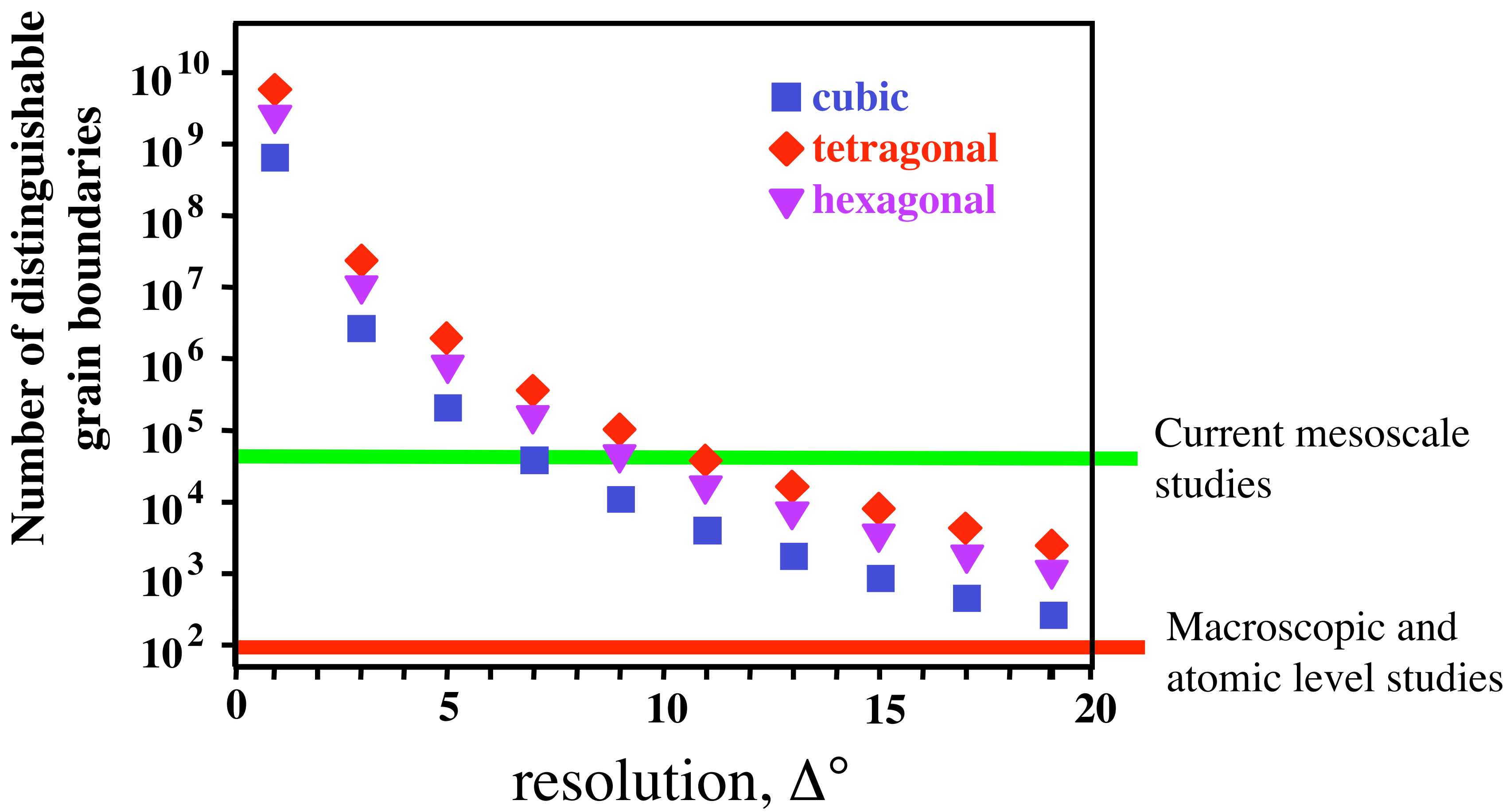

The mesoscale approach offers the opportunity to study all of the geometric possibilities

Measuring the five boundary parameters

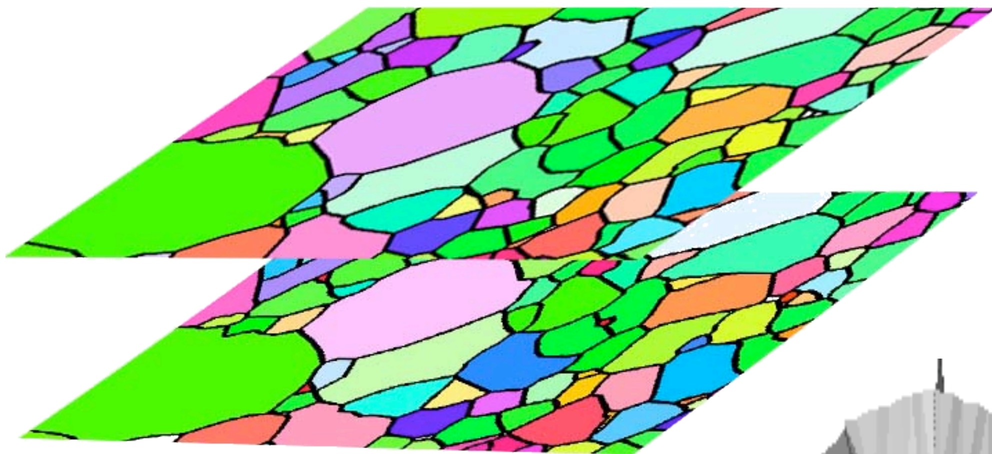

Record high resolution EBSP maps on two adjacent layers.

Assume triangular planes connect boundary segments on the two layers.

Δg and **n** can be specified for each triangular segment

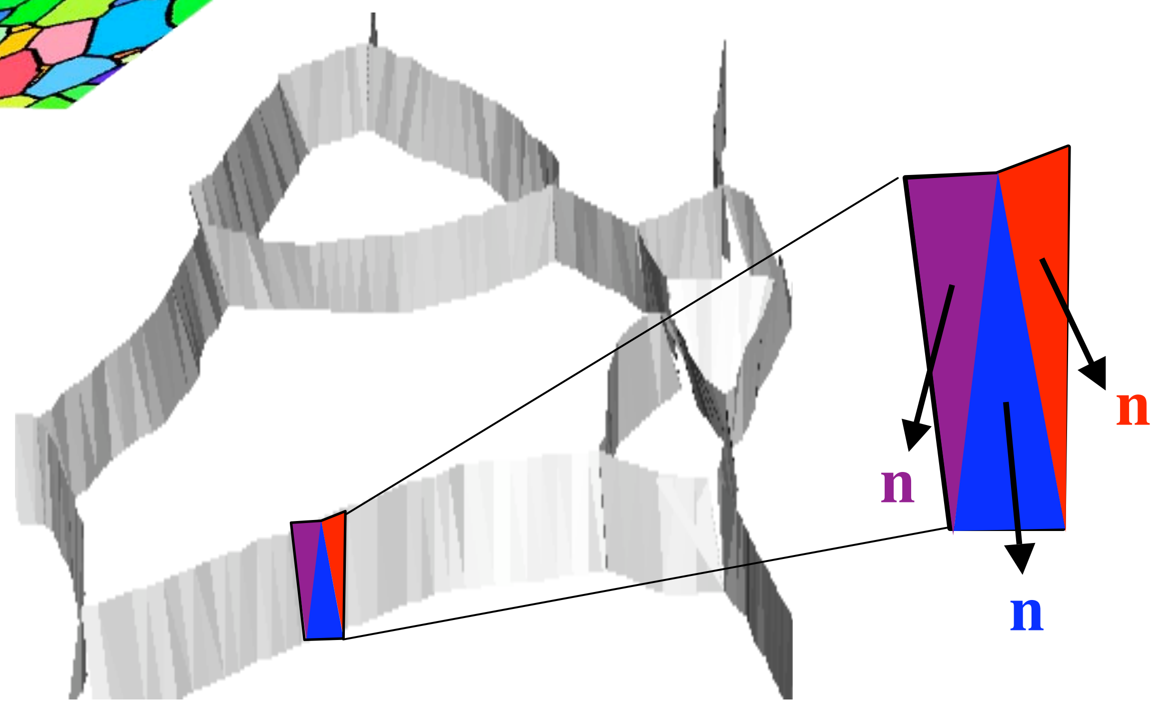

Saylor, Morawiec, Rohrer, Acta Mater. 51 (2003) 3663

2-parameter distributions: boundary normal only

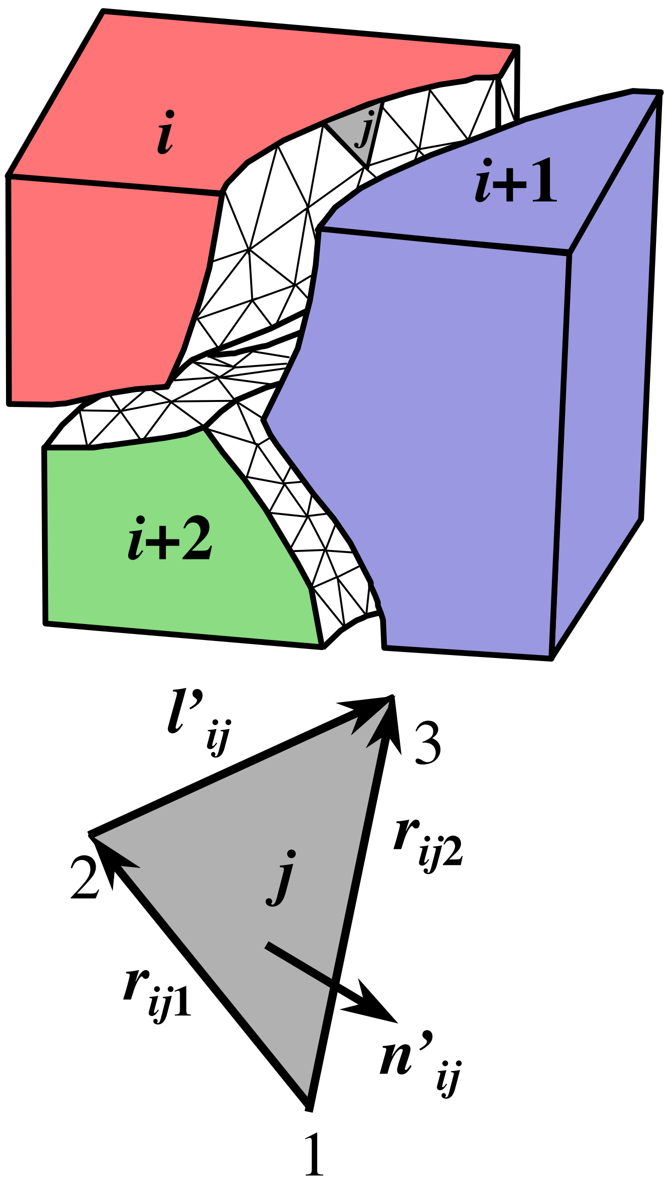

- **Index *n*' in the crystal reference frame:**
  $n = g_i n'$ and $n = g_{i+1} n'$
  (2 parameter description)

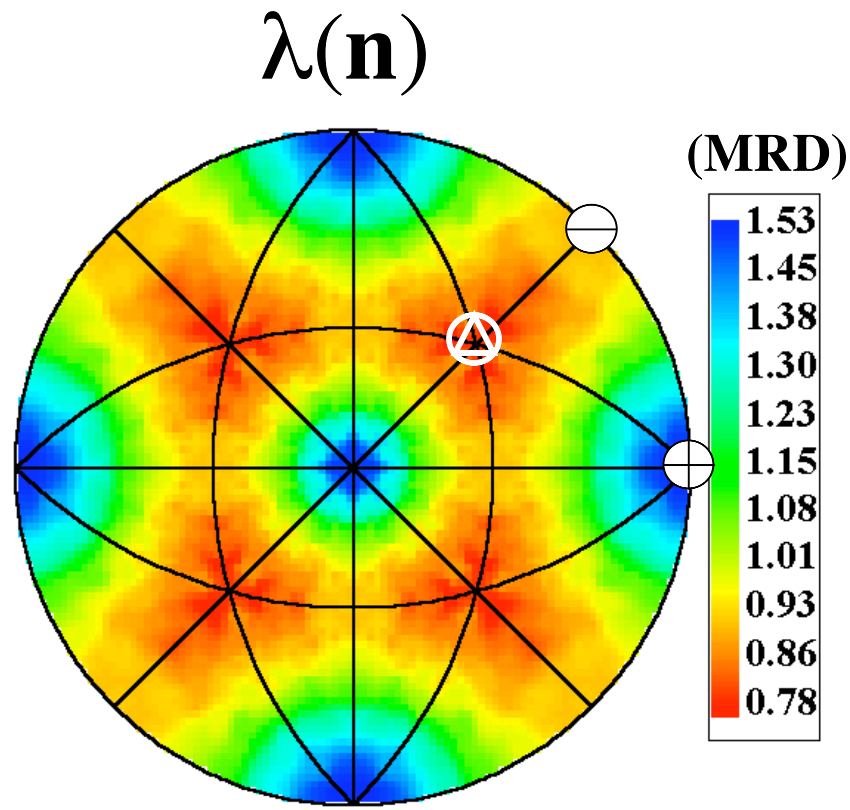

Grain Boundary Distribution in MgO: [100]

λ(Δg, **n**)

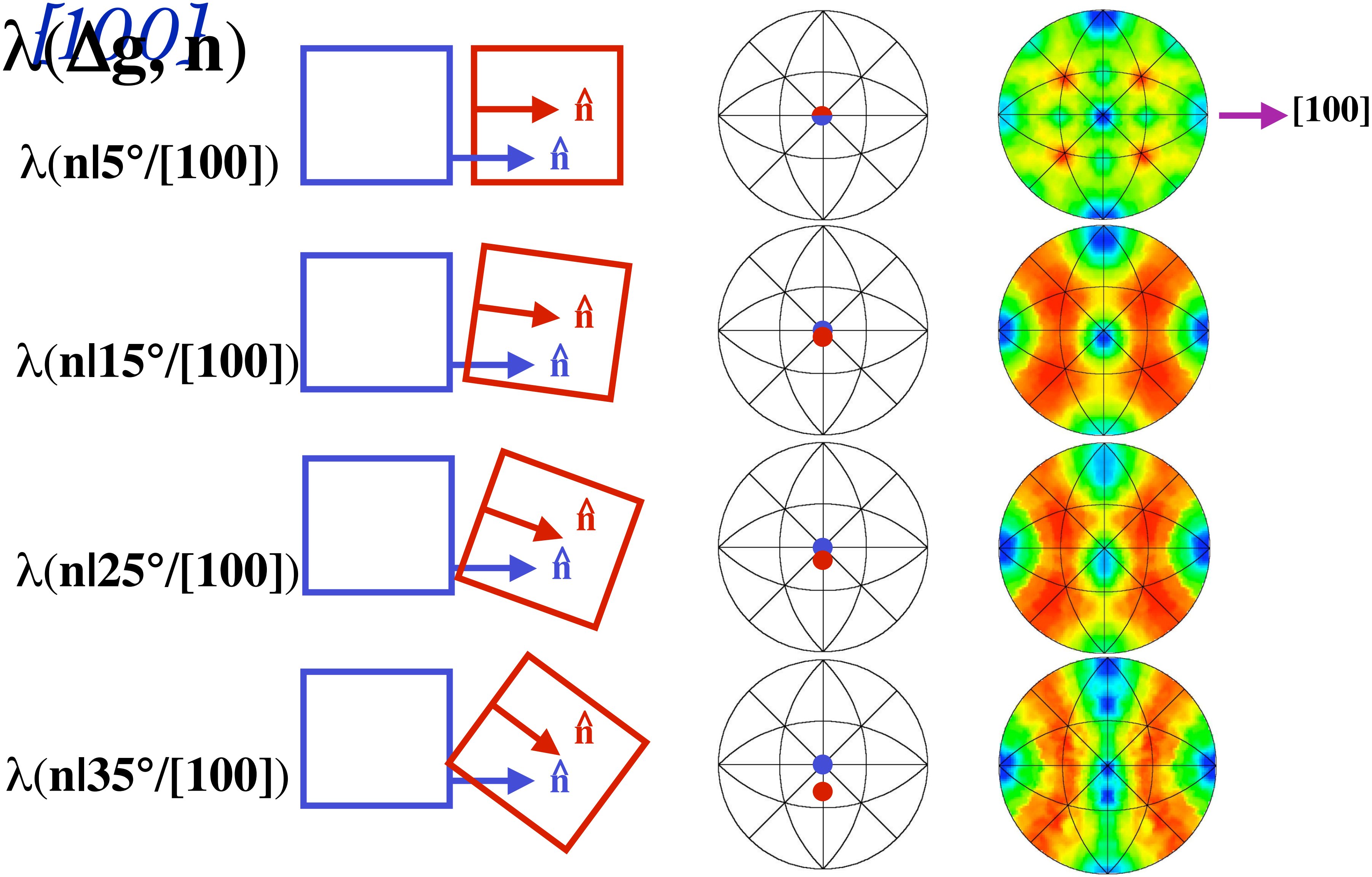

Every peak in λ(Δg,**n**) is related to a boundary with a {100} plane

Stereology for measuring Δg and n

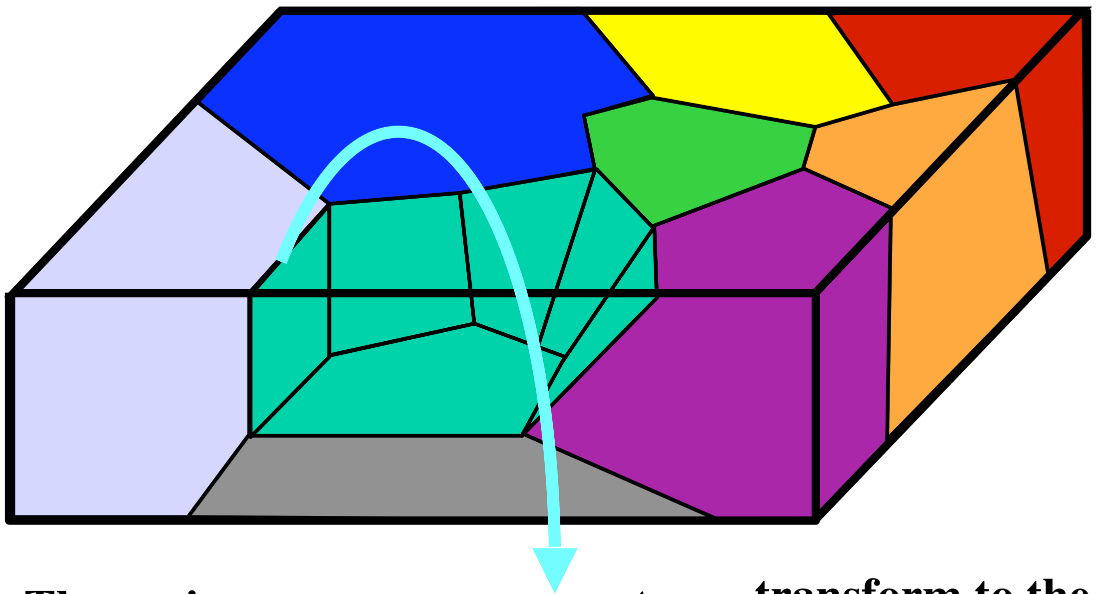

The probability that the correct plane is in the zone is 1.

The probability that all planes are sampled is < 1.

The grain boundary surface trace is the zone axis of the possible boundary planes.

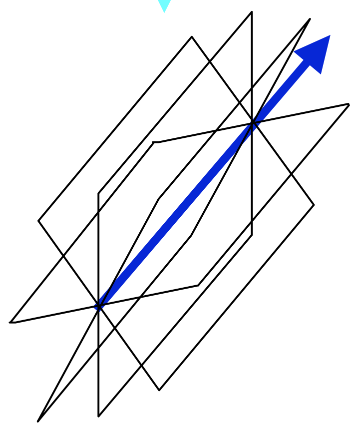

transform to the misorientation reference frame

Δg

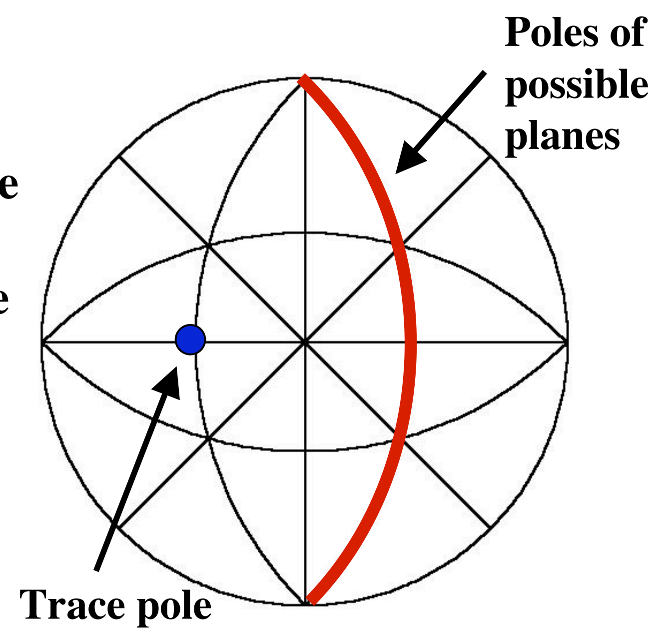

D.M. Saylor, B.L. Adams, G.S. Rohrer, "Measuring the Five Parameter Grain Boundary Distribution From Observations of Planar Sections," *Metall. Mater. Trans.*, **35A** (2004) 1981-89.

Illustration of Boundary Stereology

Grain boundary traces in sample reference frame

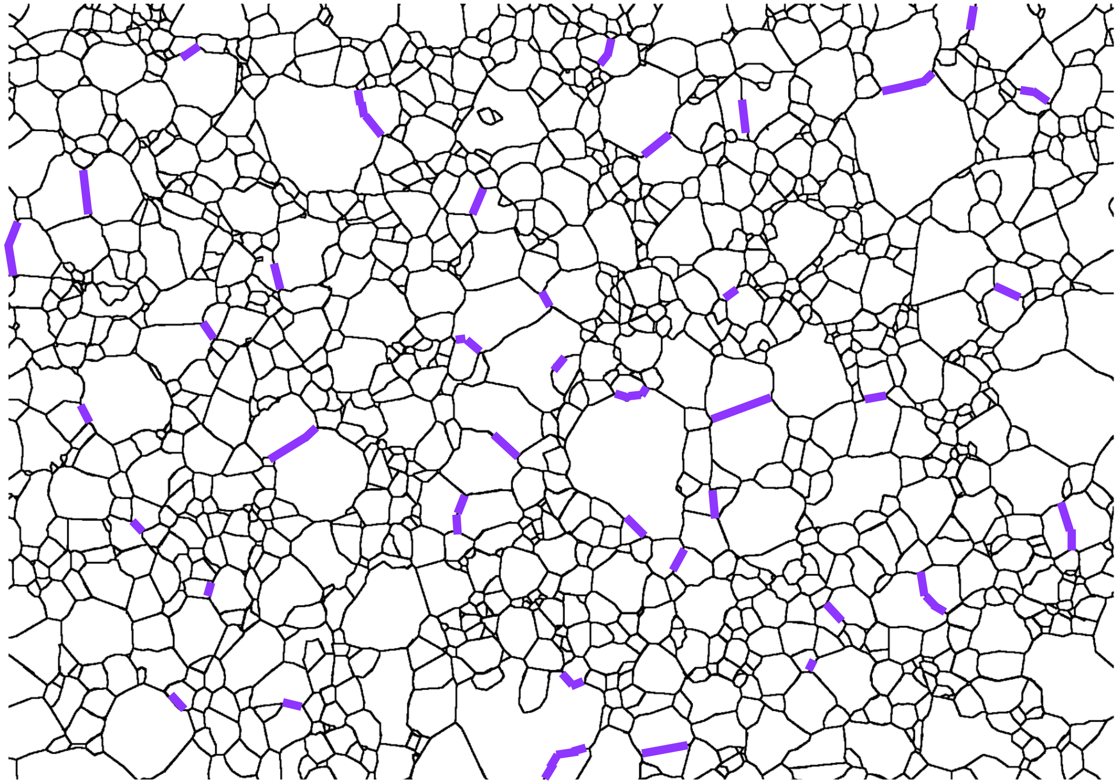

All planes in the zone of trace, in the misorientation frame (at a fixed Δg)

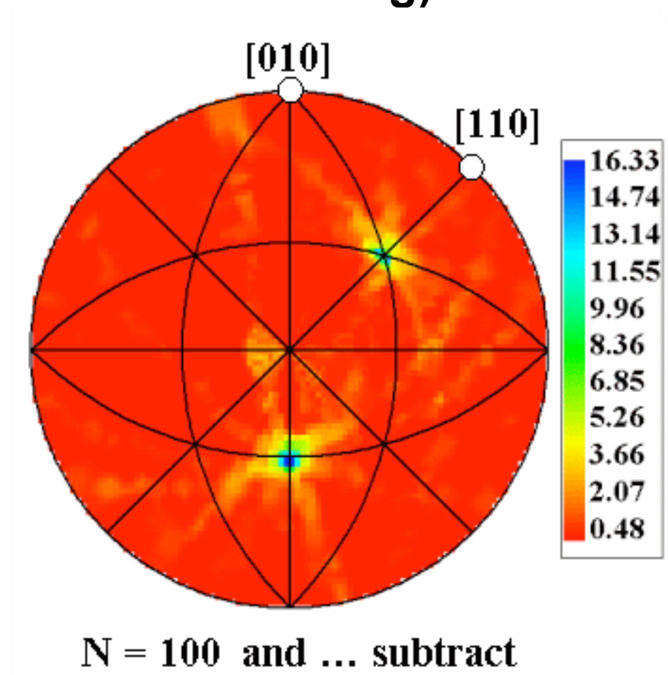

The background of accumulated false signals must then be subtracted.

- **The result is a representation of the true distribution of grain boundary planes at each misorientation.**
- **A continuous distribution requires roughly 2000 traces for each Δg**

Outline

- Motivation for studying grain boundaries
- ~~Coincident Site Lattice theory~~, or, Average Surface Energy?
- Grain boundary mobility
- Integration of properties and evolution
- Overview of grain boundary properties

Examples of 2-Parameter Distributions

Grain Boundary Plane Population (Δg averaged)

Measured Surface Energies

MgO

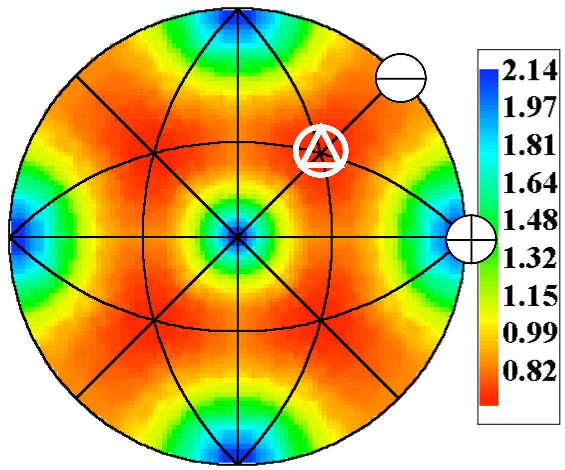

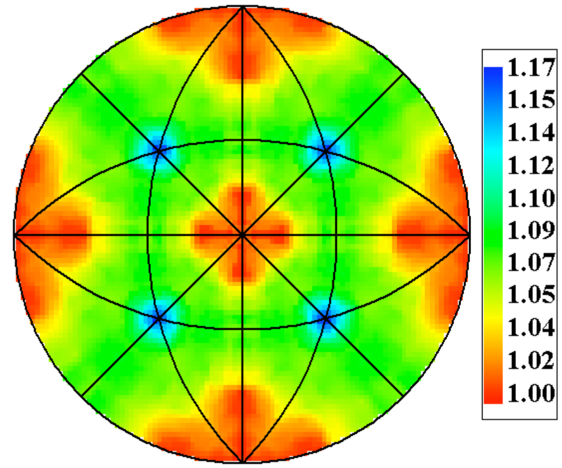

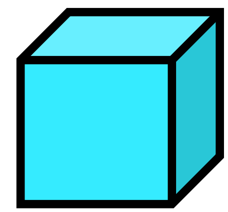

Saylor & Rohrer, Inter. Sci. 9 (2001) 35.

$SrTiO_3$

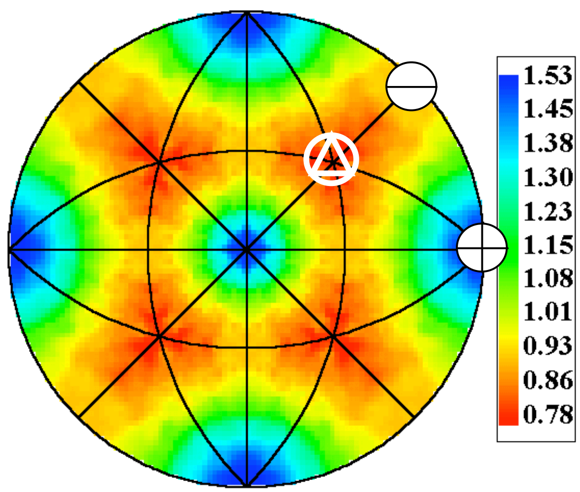

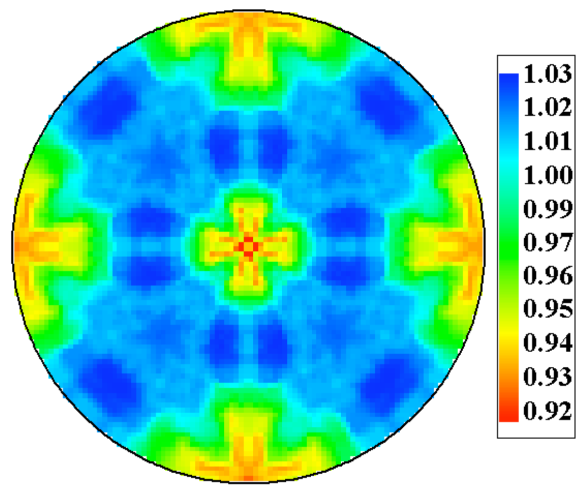

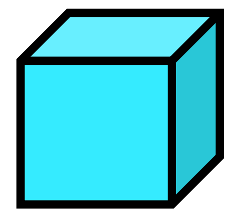

Sano et al., J. Amer. Ceram. Soc., 86 (2003) 1933.

Examples of Two Parameter Distributions

Grain Boundary Plane Population (Δ*g* averaged)

Measured Surface Energies

Al

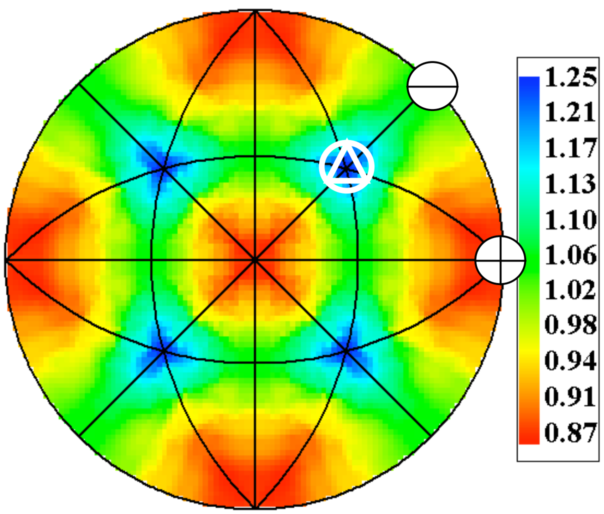

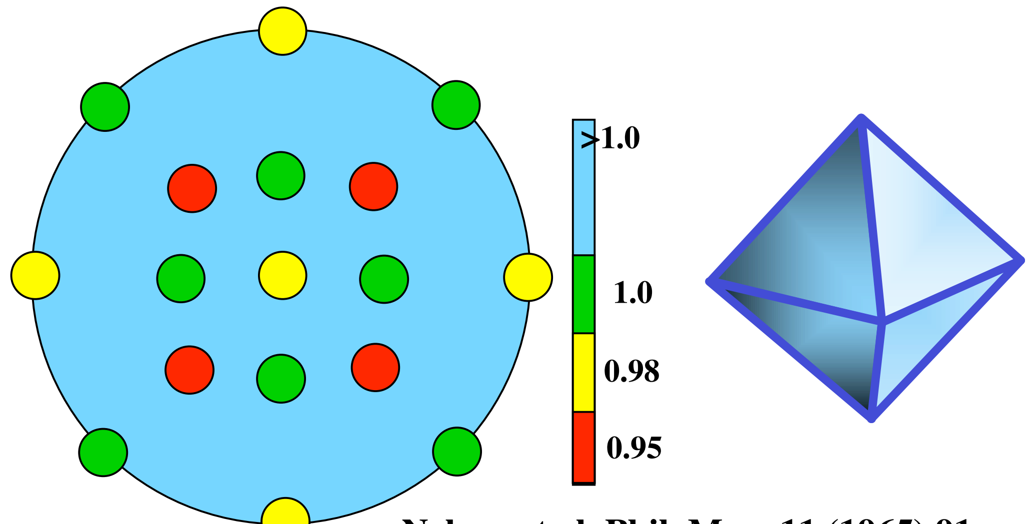

Saylor et al. *Acta mater.* **51,** (2004) 3363.

Nelson et al. Phil. Mag. 11 (1965) 91.

Fe-Si

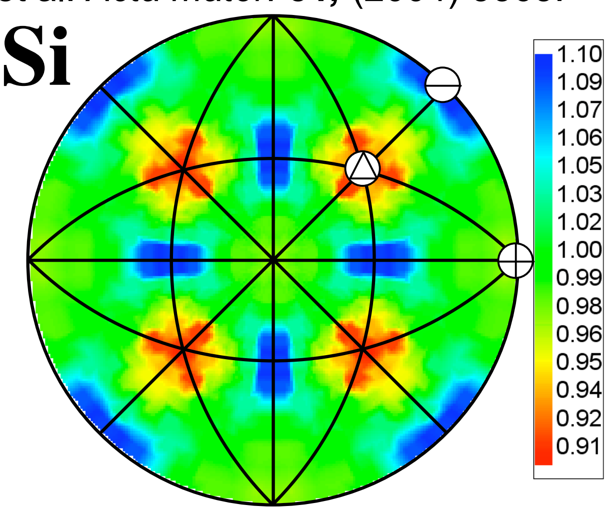

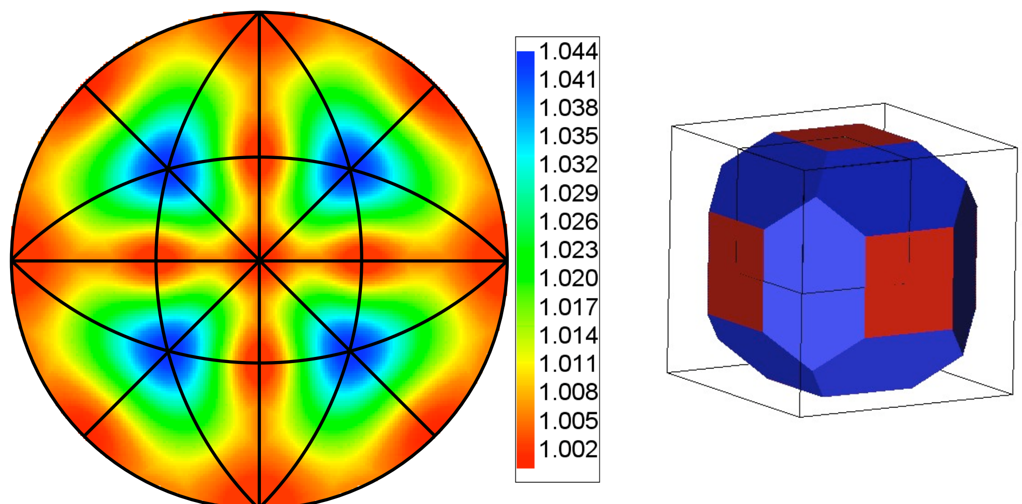

Ph.D. research, Tricia Bennett.

Gale et al. Phil. Mag. 25 (1972) 947.

Grain boundary energy and population

For all grain boundaries in MgO

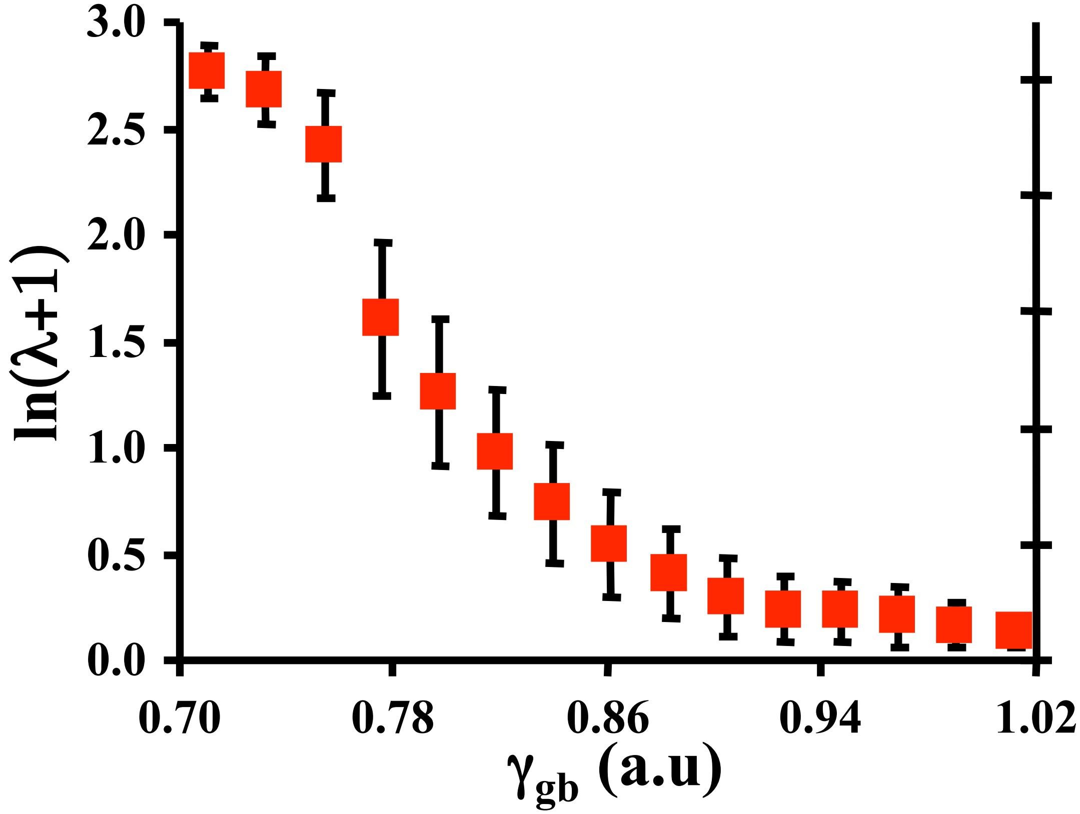

Population and Energy are *inversely correlated*

Grain boundary energy and population

[100] misorientations in MgO

Grain boundary energy
$\gamma(\mathbf{n}|\omega/[\mathbf{100}])$

Grain boundary distribution
$\lambda(\mathbf{n}|\omega/[\mathbf{100}])$

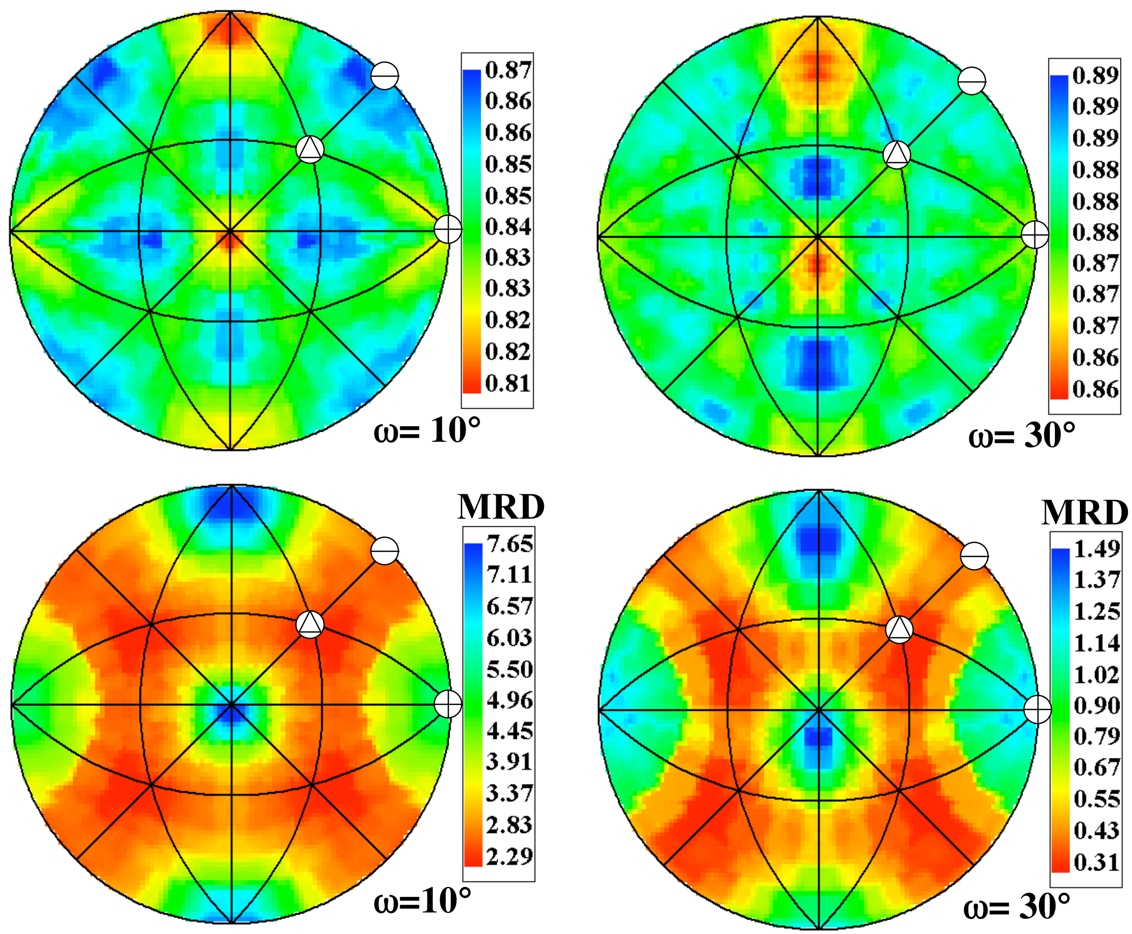

Population and Energy are inversely correlated

Saylor, Morawiec, Rohrer, Acta Mater. 51 (2003) 3675

Boundary energy and population in Al

Symmetric [110] tilt boundaries

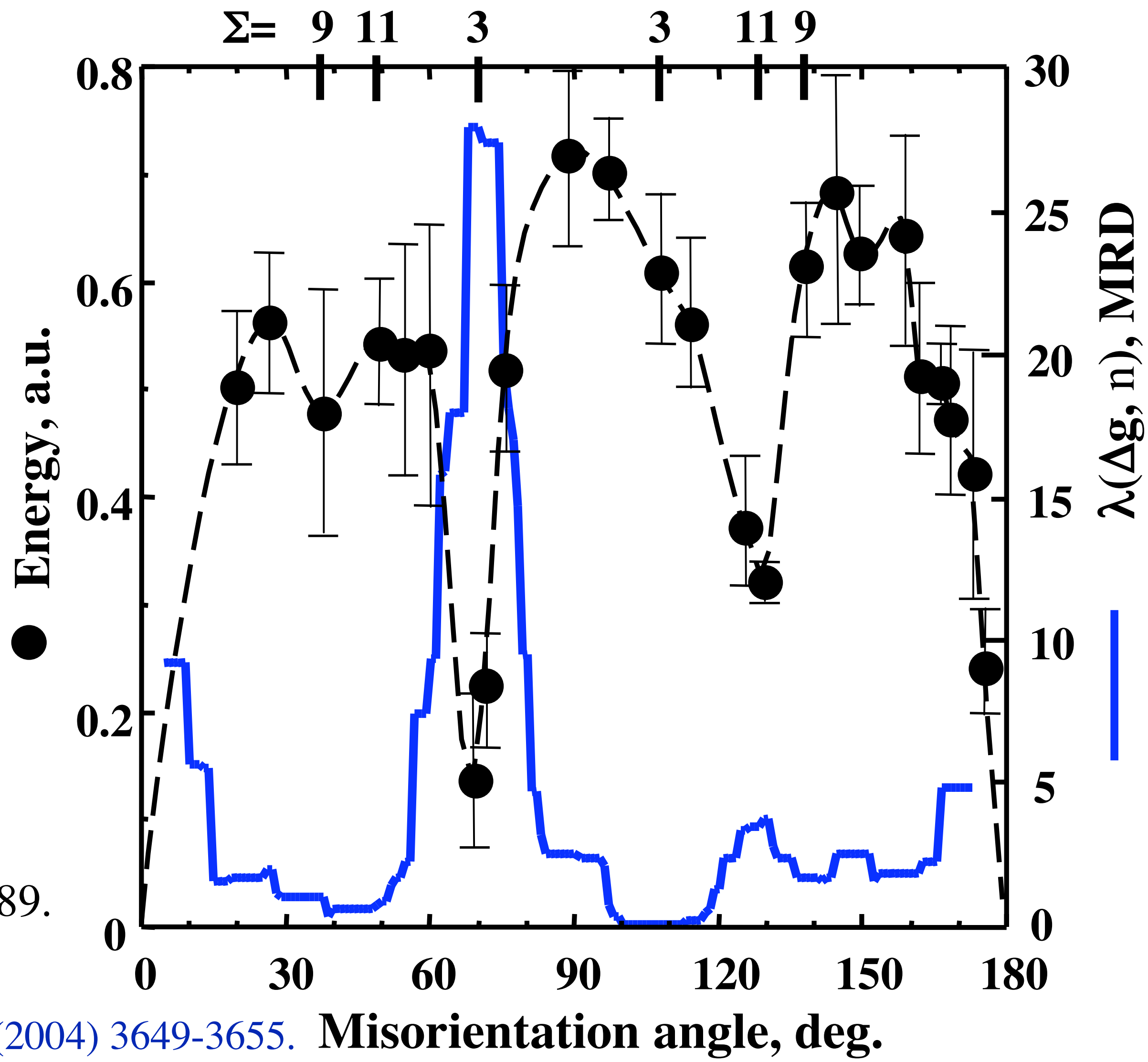

Energies:

G.C. Hasson and C. Goux *Scripta metall*. **5** (1971) 889.

Al boundary populations:
Saylor et al. *Acta mater*. **52**, (2004) 3649-3655.

Σ5 (37°/[100]) tilt boundaries in MgO

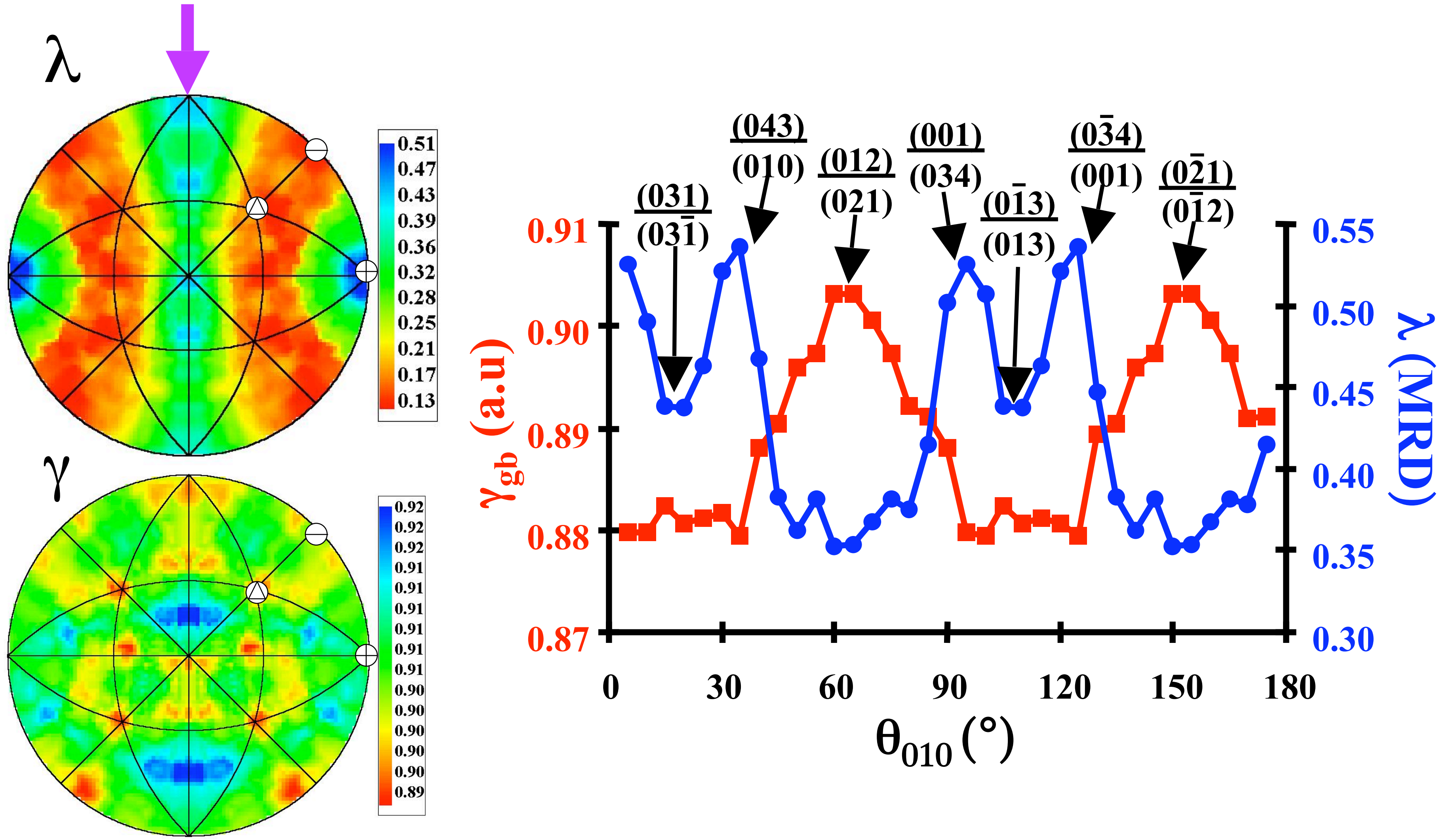

The energy-population correlation is not one-to-one

$\lambda(n)$ for low Σ CSL misorientations: $SrTiO_3$

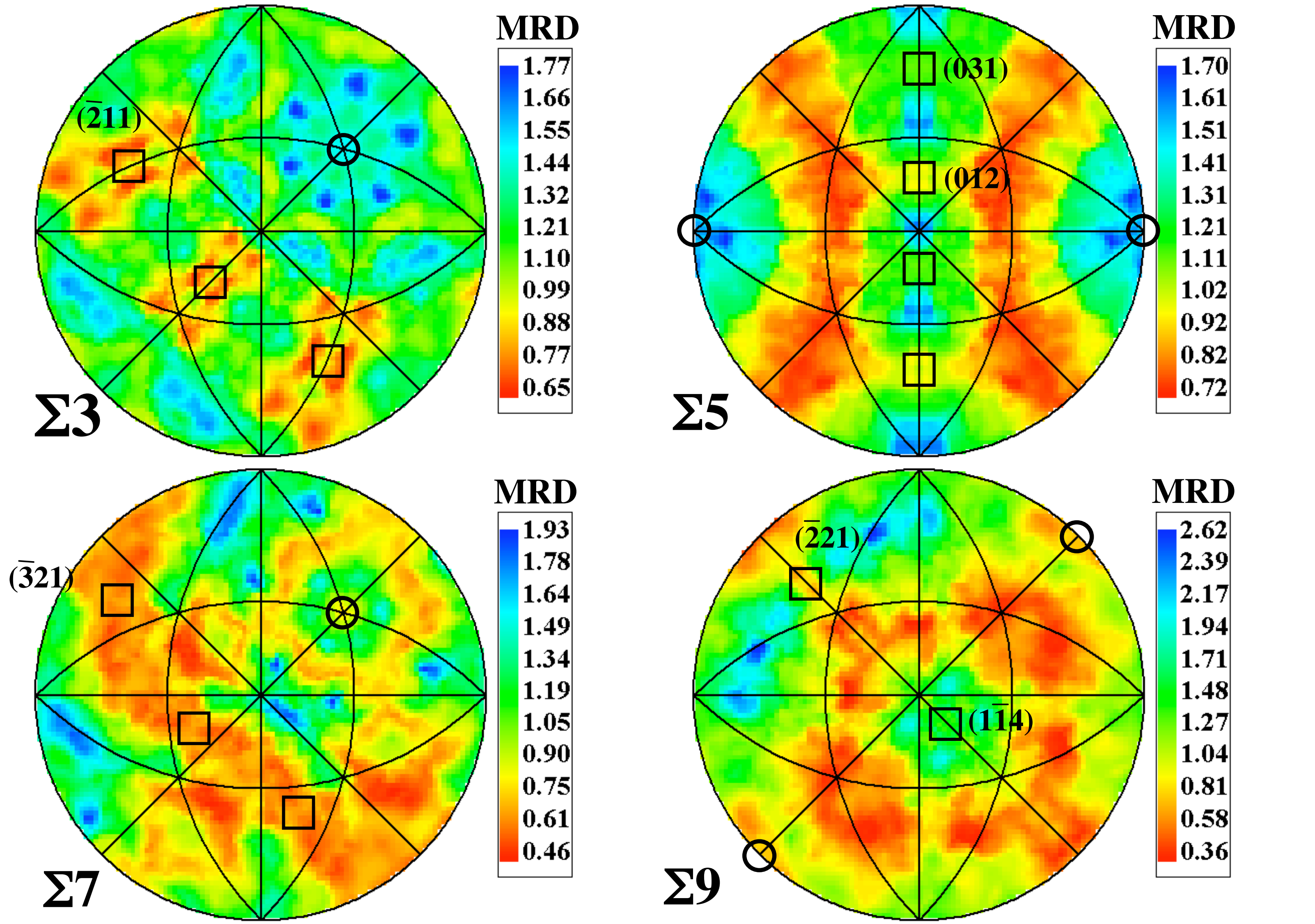

Except for the coherent twin, a high density of coincident lattice sites in the boundary plane does *not* explain the variations in the grain boundary population.

Grain Boundary Distribution in Al: {111} axes

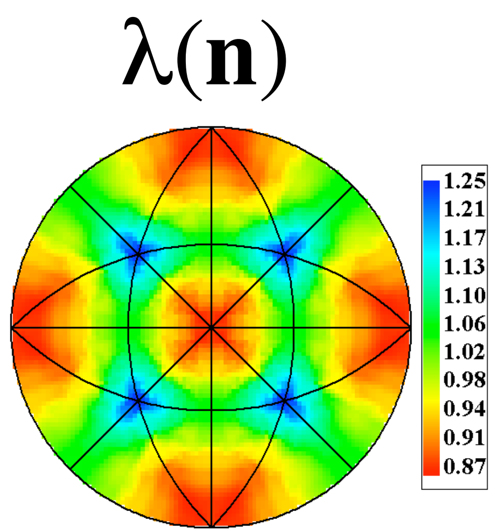

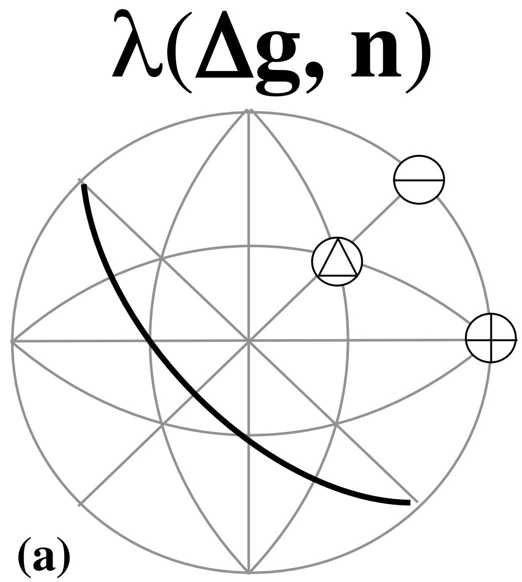

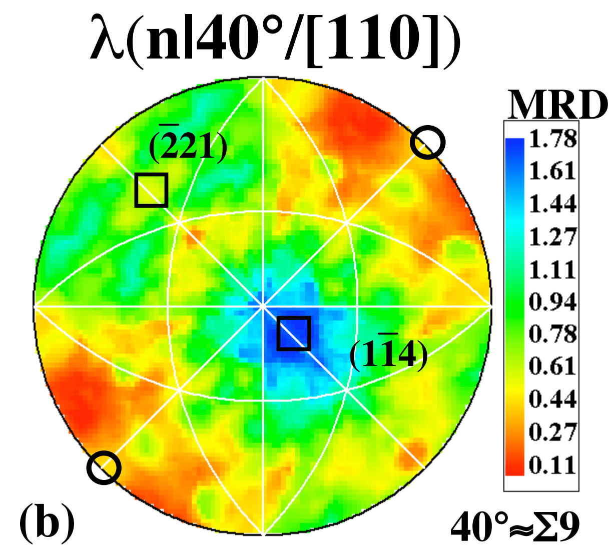

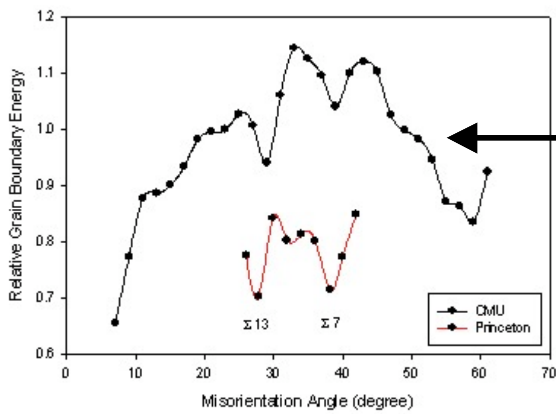

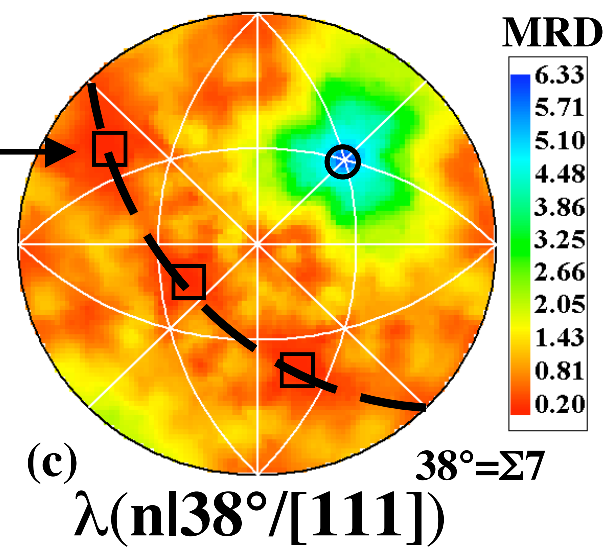

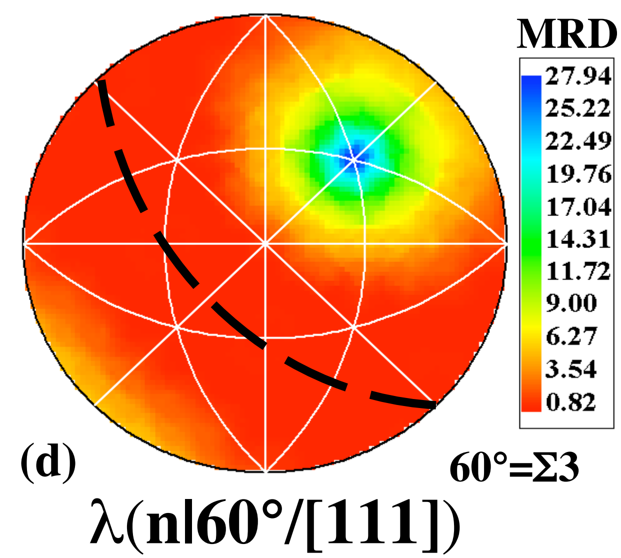

<111> tilt boundaries analyzed in an Al thin film, annealed at 400°C.

(111) Twist boundaries are the dominant feature in $\lambda(\Delta g,\mathbf{n})$

Grain Boundary Distribution in Al: [111] misorientation axes

<111> tilt boundaries analyzed in an Al thin film, annealed at 400°C (Archibald, Kim & Kim). Minima in measured g.b. energy correspond to the results of MD calculations (Srolovitz, Princeton).

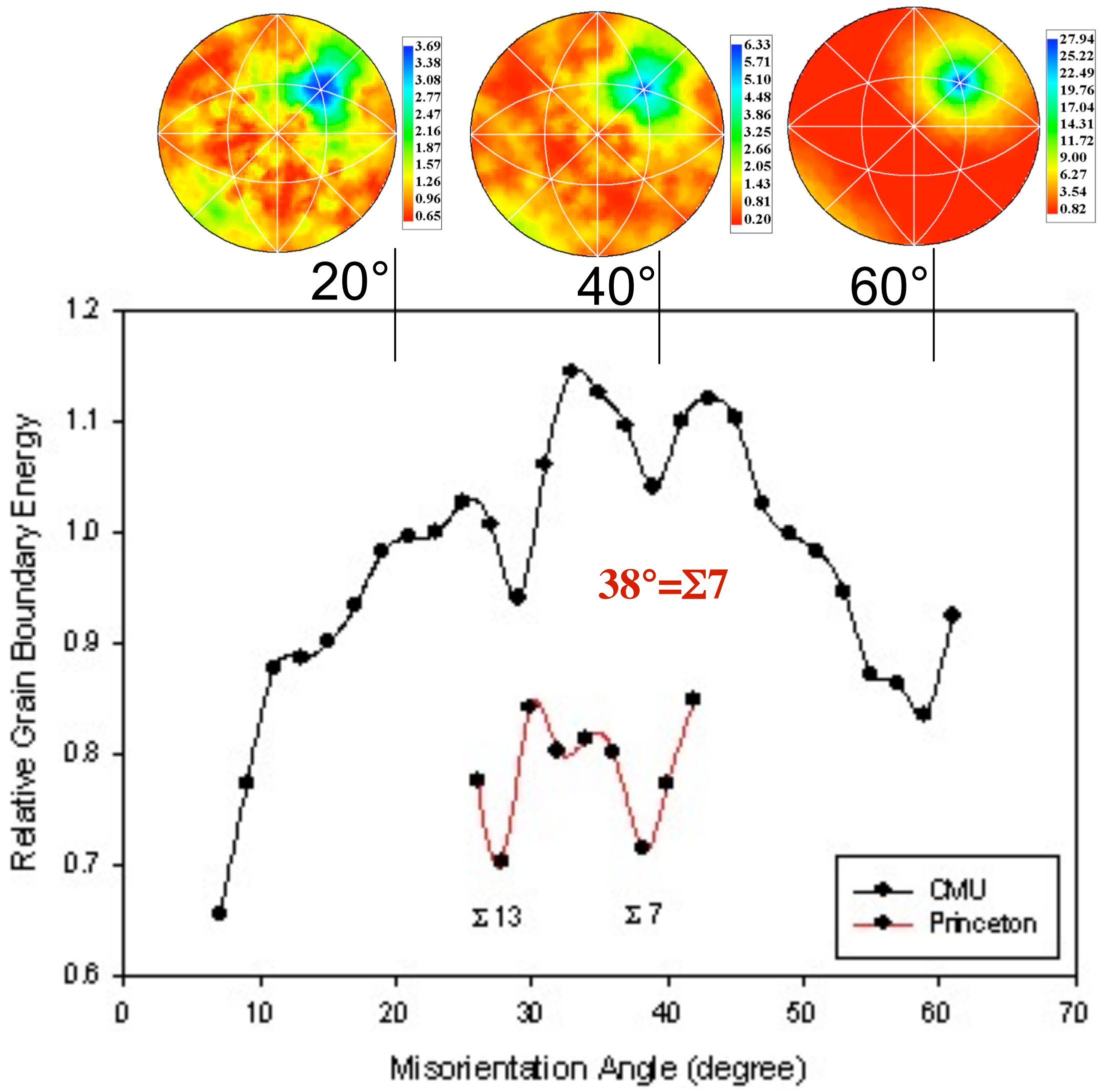

Grain Growth Simulations with Grain 3D

A.P. Kuprat: *SIAM J. Sci. Comput*. **22** (2000) 535. **G**radient **W**eighted **M**oving **F**inite **E**lements (LANL); PhD by Jason Gruber

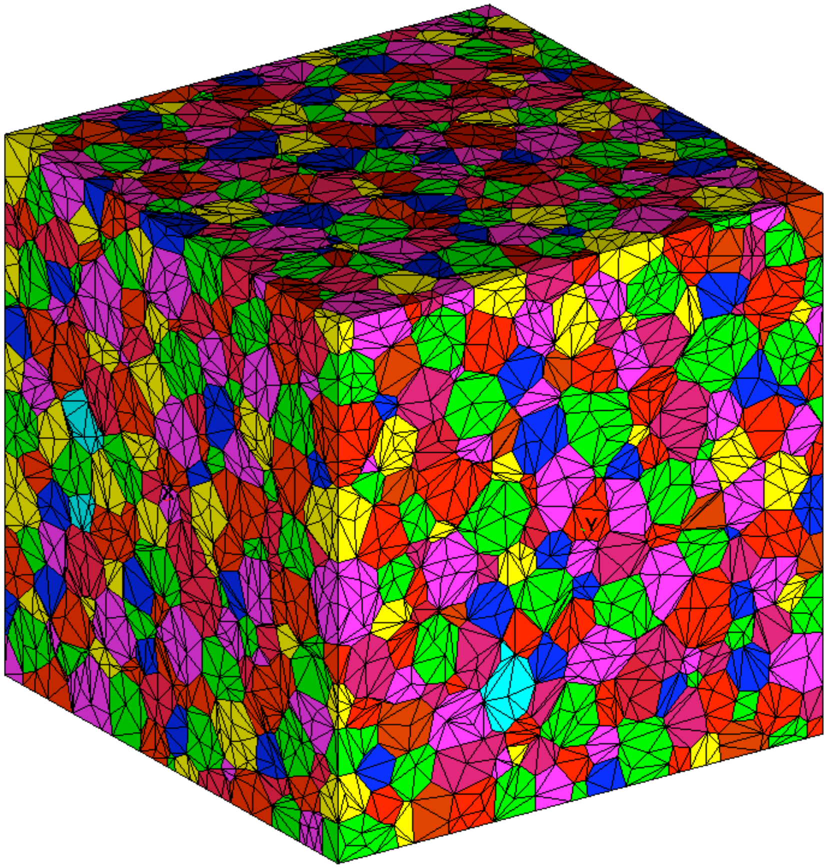

Elements move with a velocity that is proportional to the mean curvature

Initial mesh: 2,578 grains, random grain orientations (16 x 2,578 = 41,248)

Use input energy function modeled after that observed for magnesia.

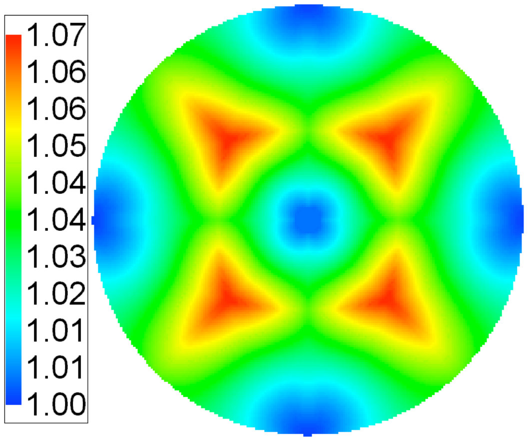

Grain 3D Simulations

- Input energy modeled after MgO
- Steady state arises that correlates with energy.

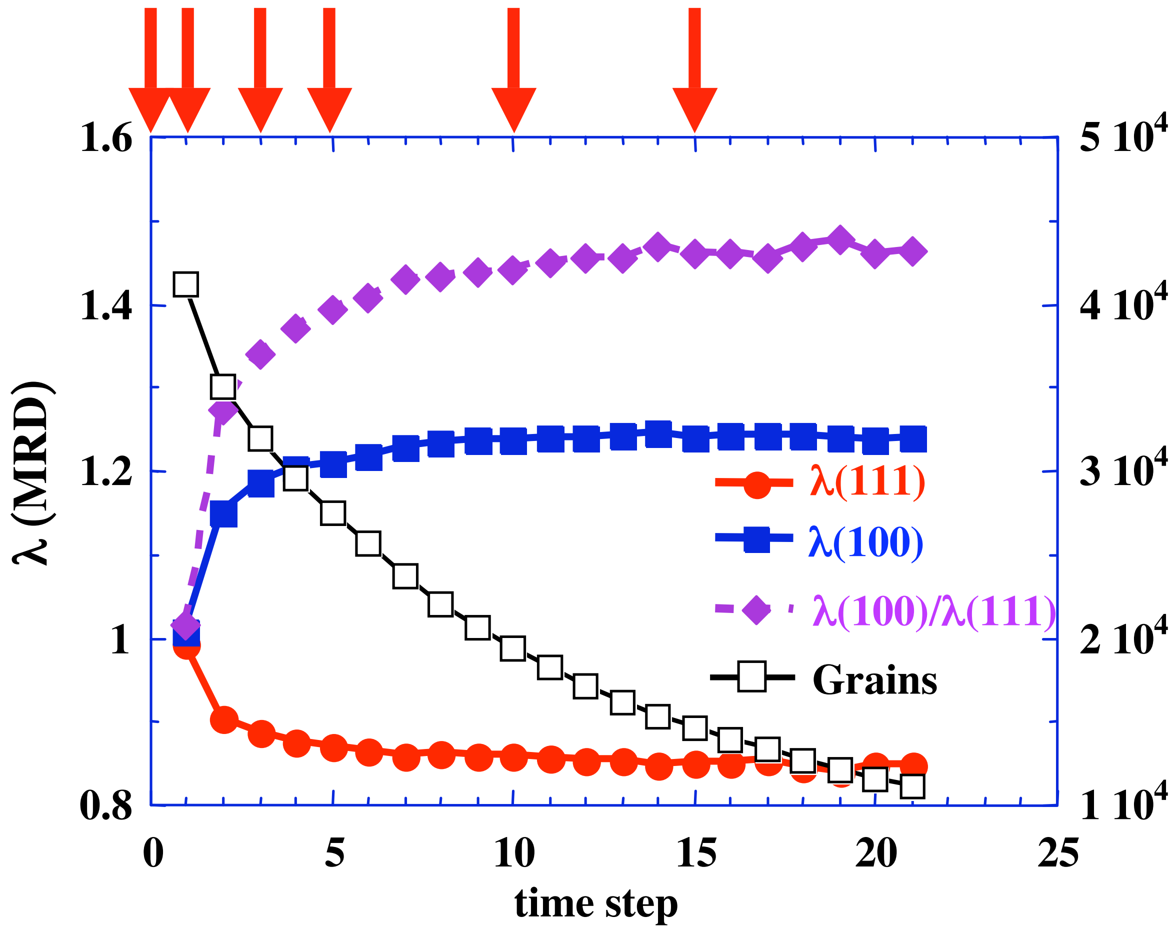

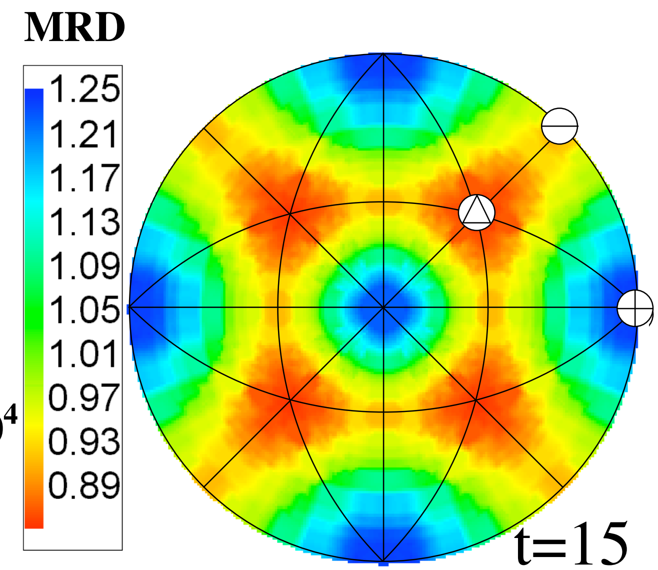

λ(n)

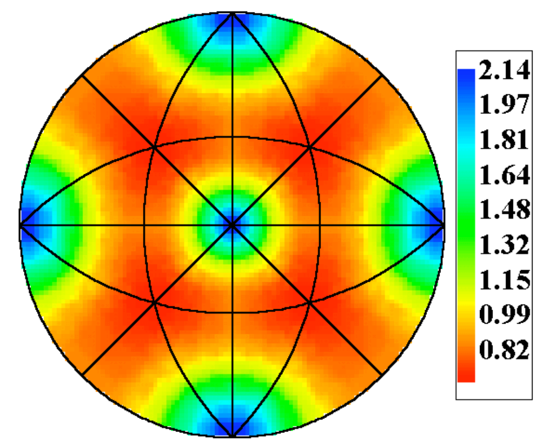

Measured versus Simulated Distributions (MgO)

25° rotation about [100].

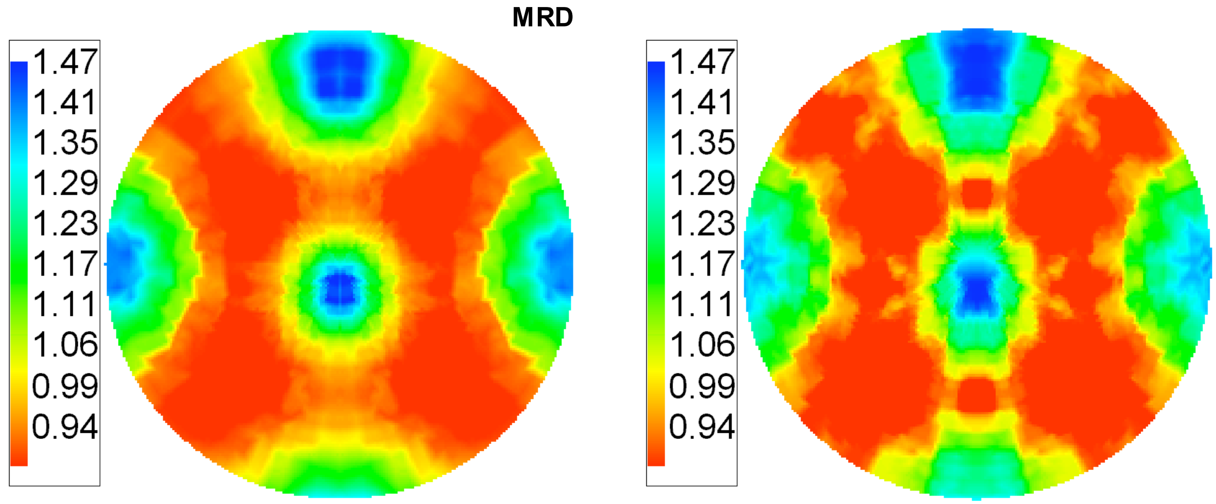

measurement[†] (left) versus simulation (right).

45° rotation about [100].

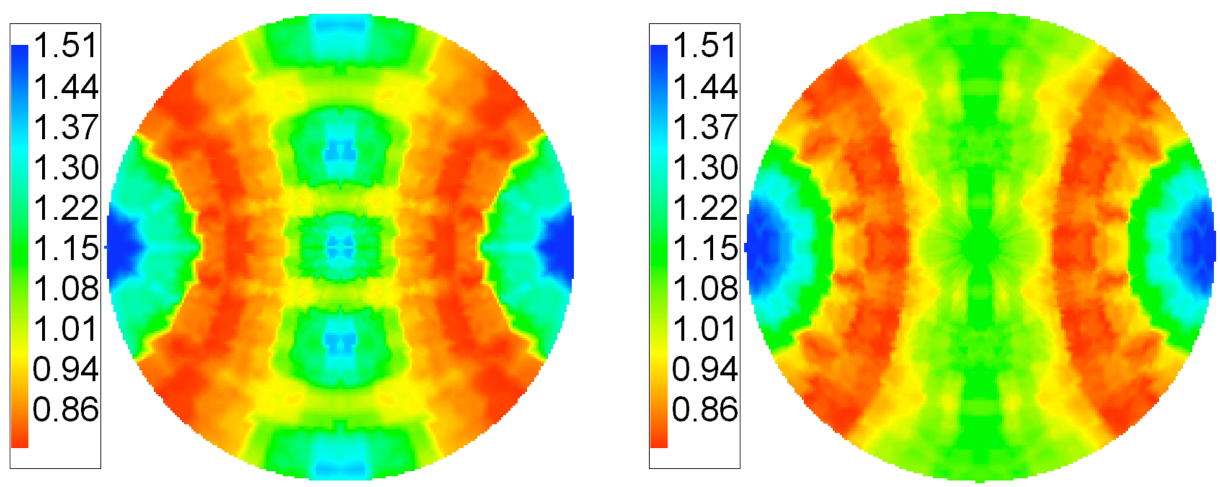

[†]Saylor et al. Acta Mater., **51** (2003) 3663-74.

G.B. populations, energy

- Statistical stereology combined with misorientation allows 5-parameter g.b. distributions to be measured without serial sectioning: c*aveat* = ~random texture required
- G.b. populations inversely correlated with g.b. energy: high energy ⇒ few, low energy ⇒ many.
- Simulation of grain growth (3D) shows development of steady state g.b. population that correlates inversely with energy anisotropy
- A broken bond model is (surprisingly) effective at explaining the observed g.b. energy anisotropy in all materials studied to date, i.e. low index planes (100 in MgO, 111 in Al, Cu, Ni) in the g.b. associated with low energy
- The CSL theory is a poor predictor of the observed g.b. energy (in contrast to the broken bond model)

Outline

- Motivation for studying grain boundaries
- ~~Coincident Site Lattice theory~~, or, Average Surface Energy?
- Grain boundary mobility
- Integration of properties and evolution
- Overview of grain boundary properties

Mobility Measurement

- PhD by Mitra Taheri
- Deform single crystals (Beck expts.);
  - scratch to promote nucleation;
  - anneal to allow growth of new grains to occur;
  - measure sizes as a function of boundary type.
- Main finding: $\Delta g = 38° \langle 111 \rangle$ is special in the sense of having high mobility (with strong normal dependence) but low activation energy. Thus at high T, the mobility advantage disappears. This corresponds to the *compensation effect* noted by Gottstein et al. for g.b. migration under a curvature driving force.

Grain Morphology: HPAl+Zr at 350ºC

- IPF images above sho
from 187 to 237 minute

- The most mobile grain
faceting and are elon

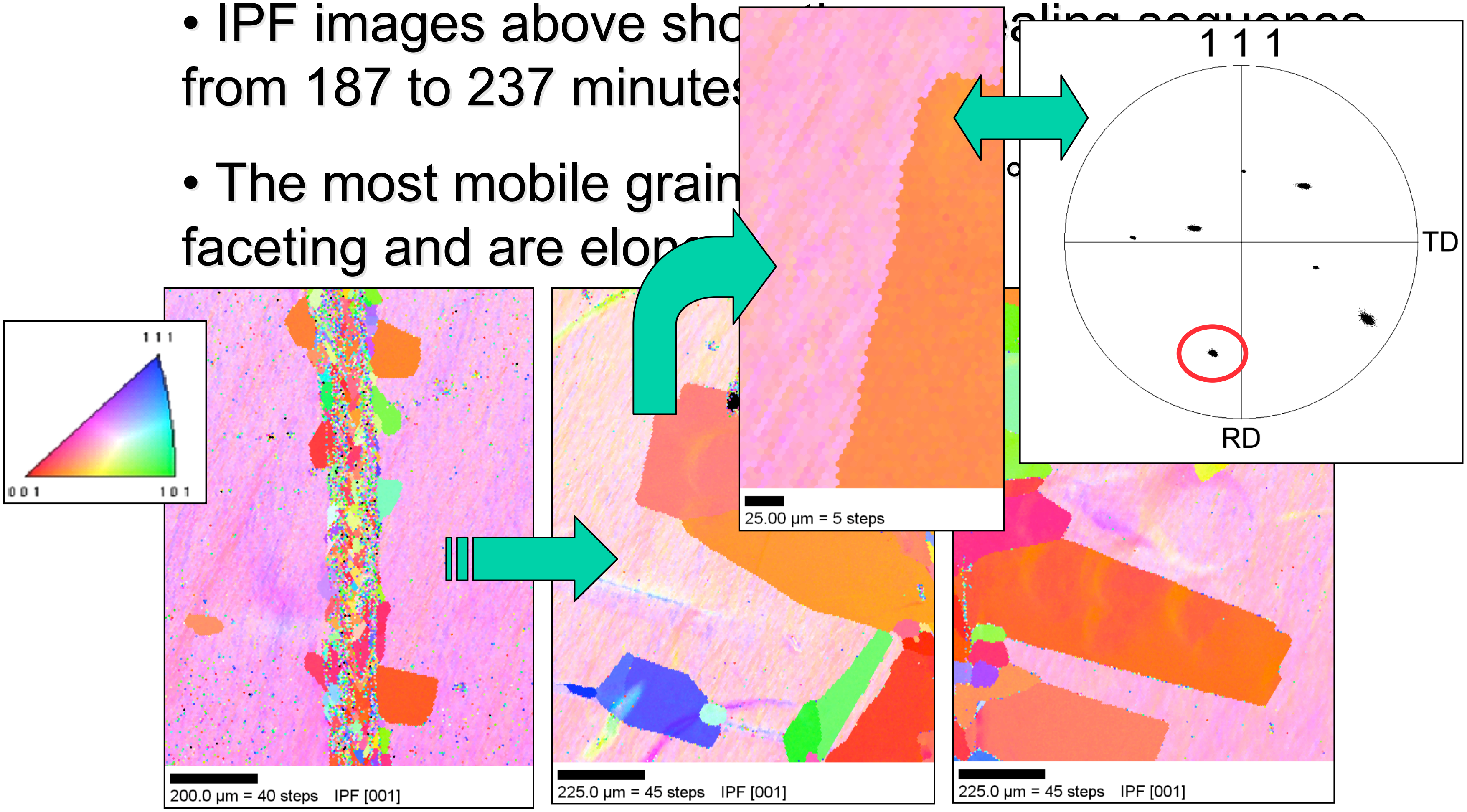

- <111> pole figure suggests that the side facets of the highly mobile 38°<111> grain are sessile pure twist boundaries (111 planes)

Grain Boundary Mobility: HPAl+Zr

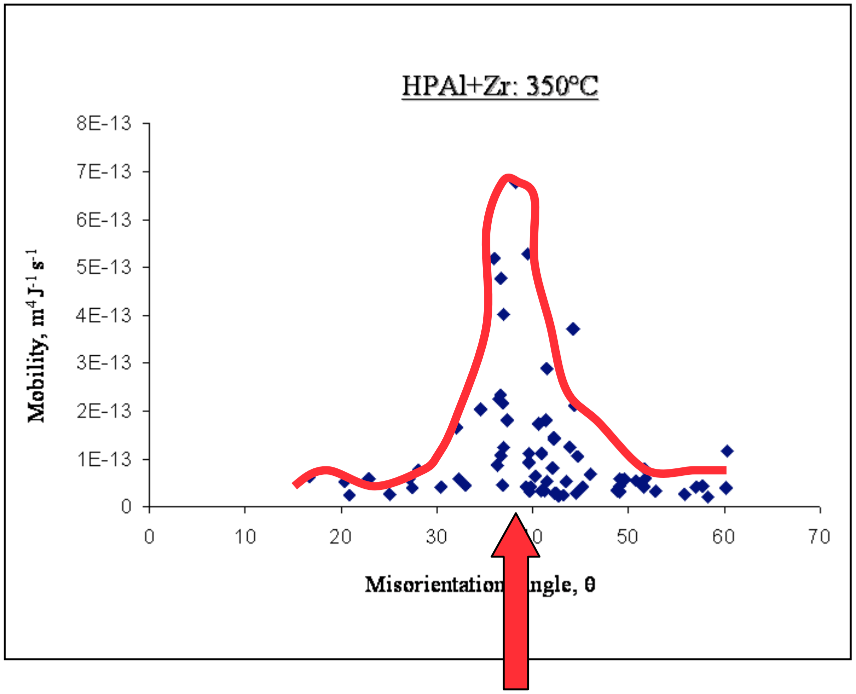

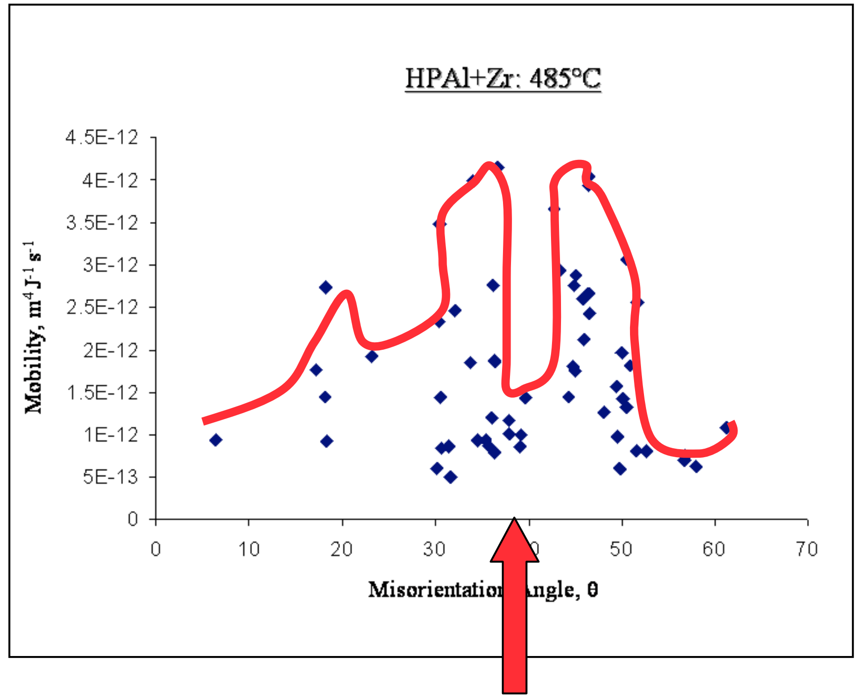

- Minimum Mobility: 2.10^{-14} $m^4J^{-1}s^{-1}$
- Minimum Mobility: 5.10^{-13} $m^4J^{-1}s^{-1}$

- Change from low to high annealing temperature results in a peak shift: maximum at 38º changes to minimum with 2 maxima at 35º and 48º

Mobility vs. Boundary Type: 350°C

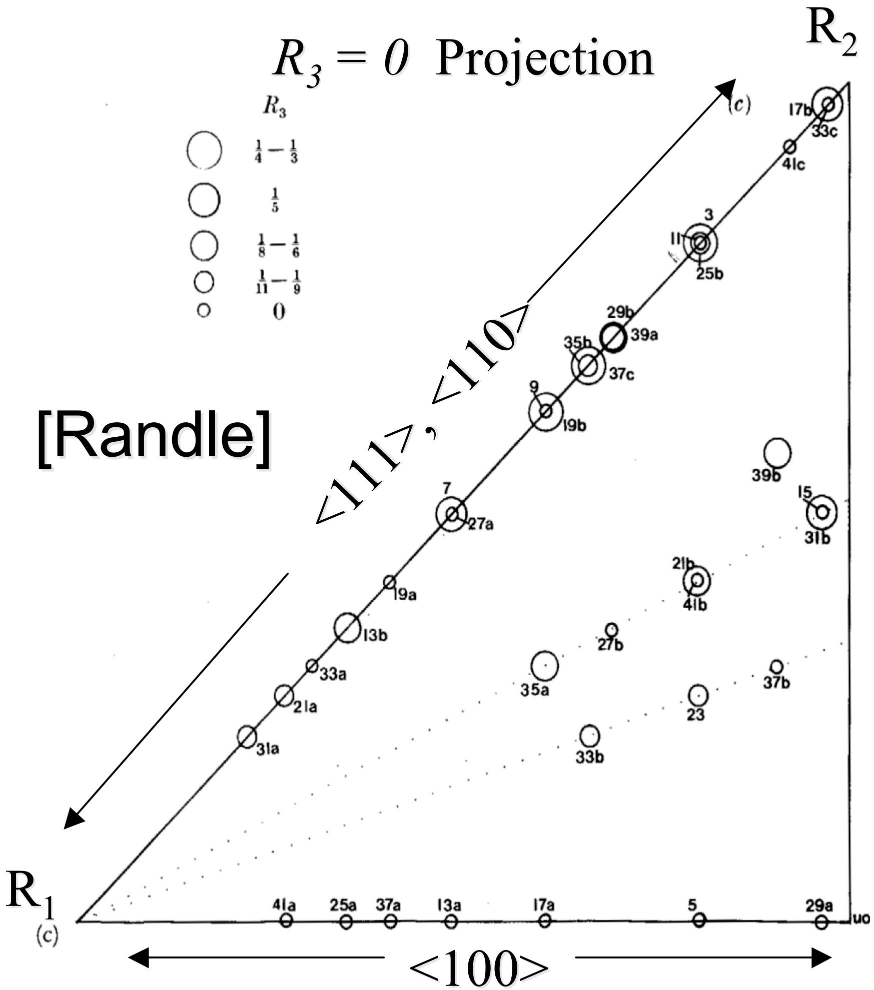

[Randle]

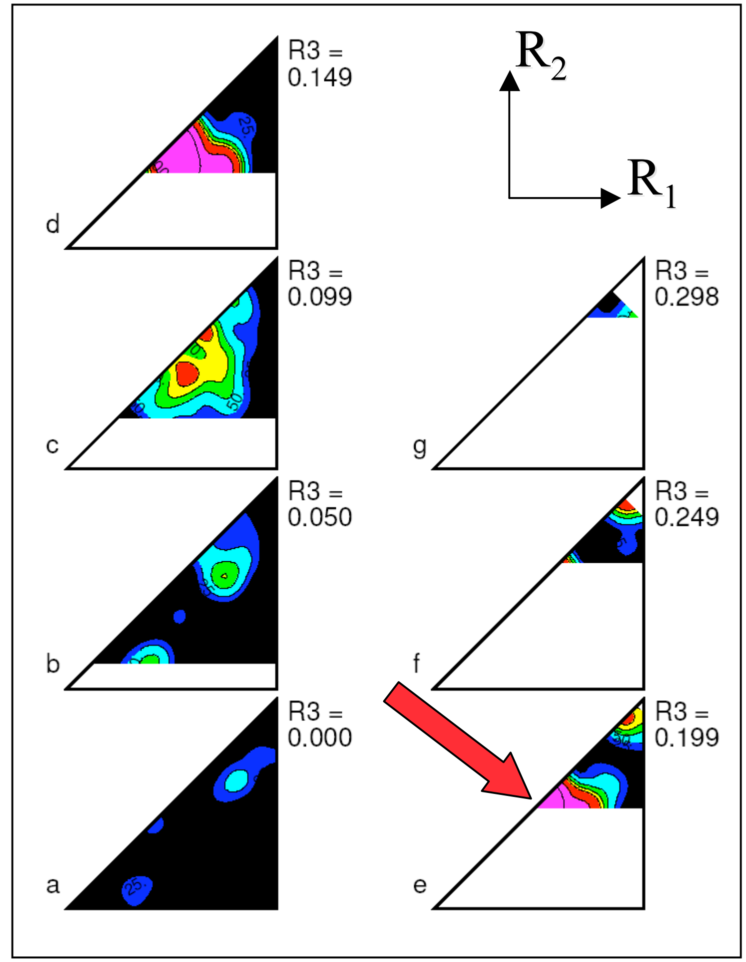

- At 350ºC, <u>only</u> boundaries close to 38°<111> are mobile

Mobility in Rodrigues space: 350 vs. 485°C

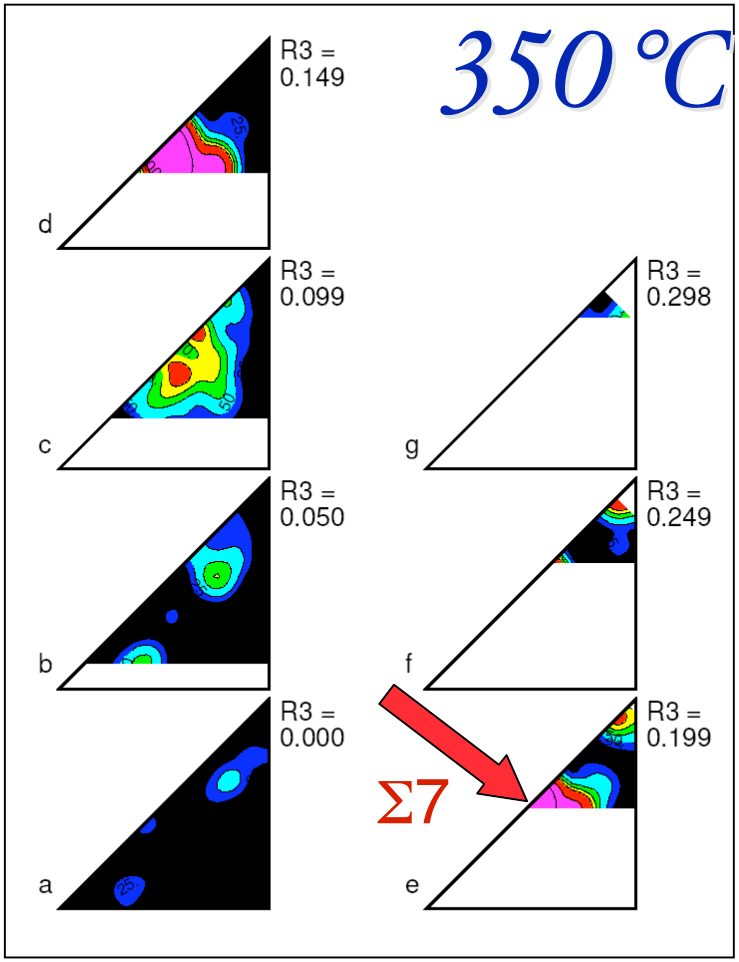

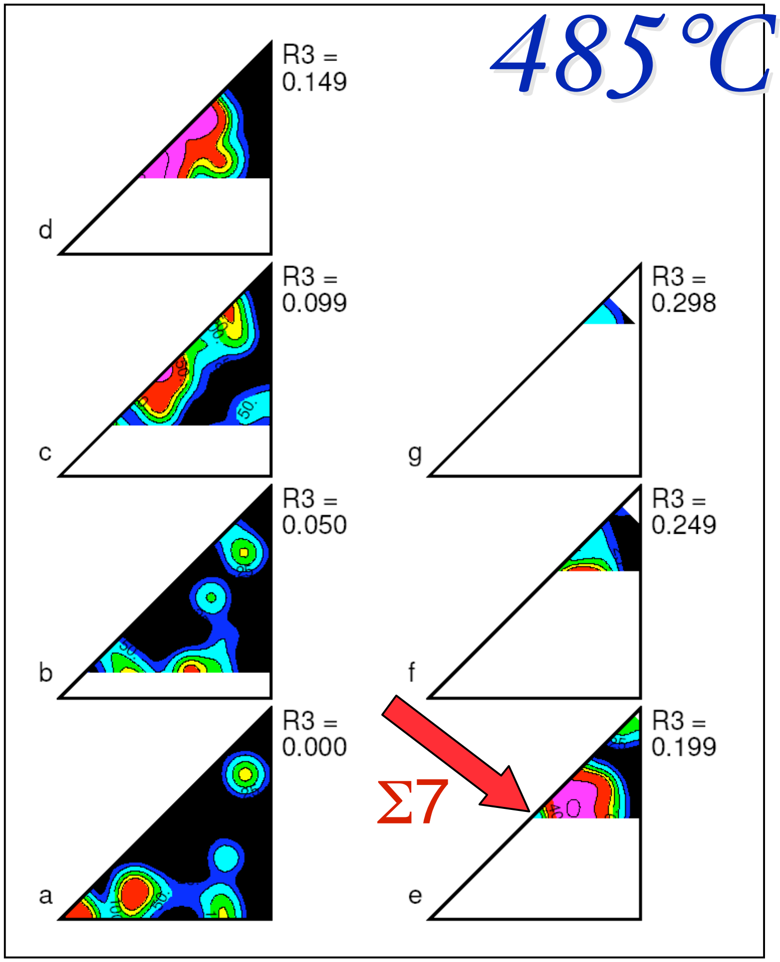

- At 485ºC, other boundary types become mobile: <100>, others, and the peak near 38°<111> splits.

Commercial Purity Al + Zr

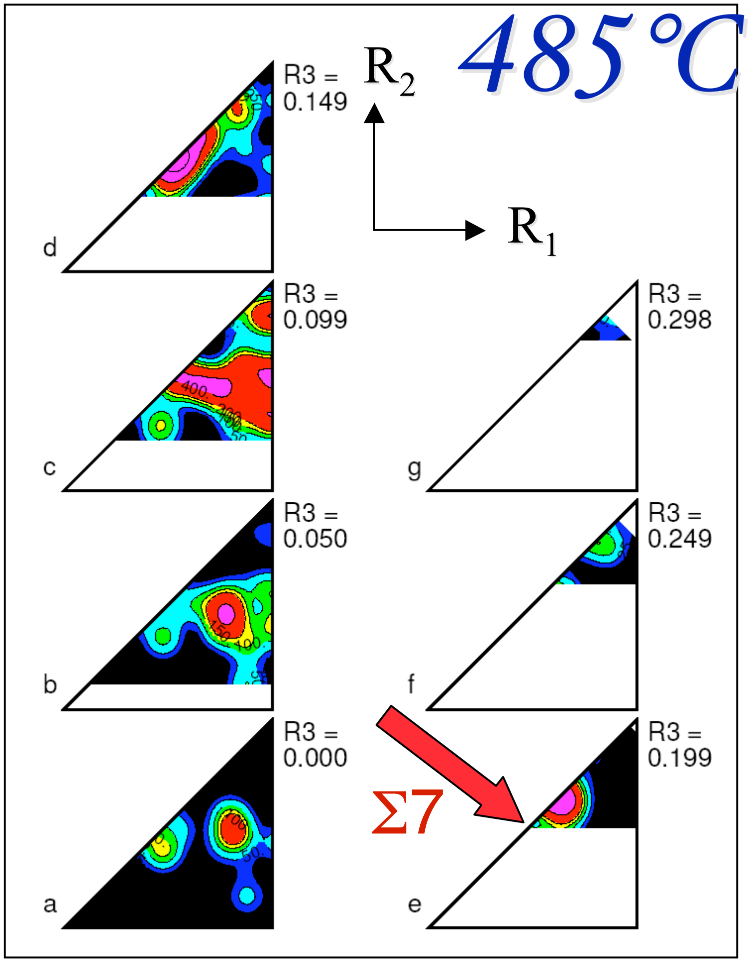

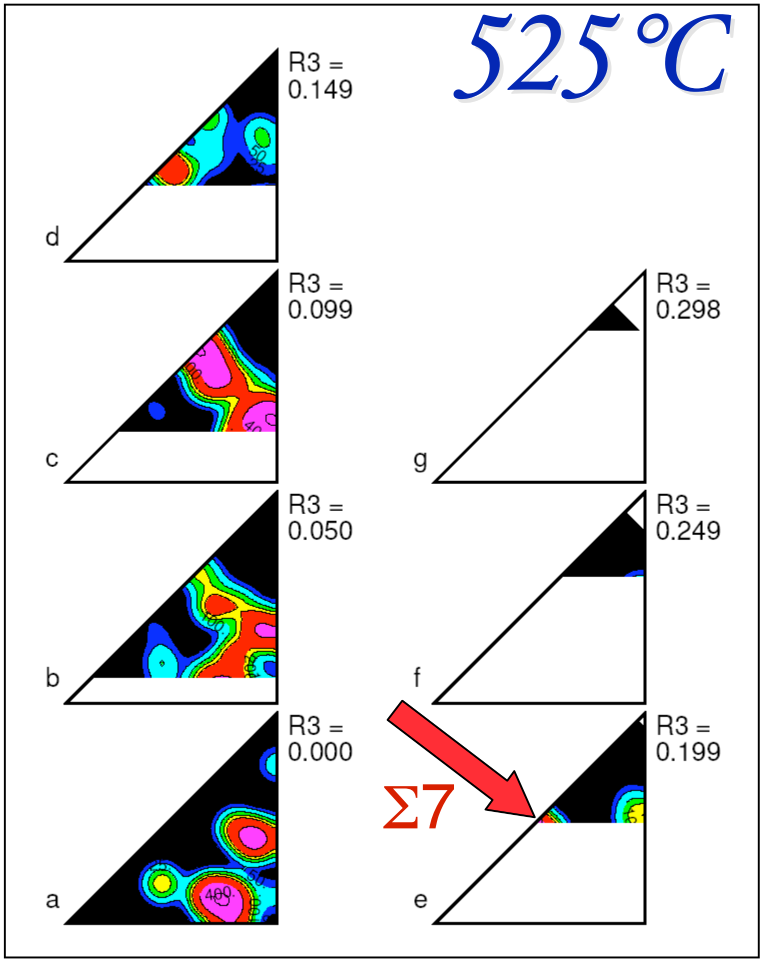

Broad range of mobile boundary types, with peaks near <111>.

Some near-<100> mobility appears, with minor 38°<111> peak.

Compensation Effect

Both *curvature* and *stored energy* driving forces appear to yield similar results. The apparent activation enthalpy varies significantly, leading to a "compensation effect."

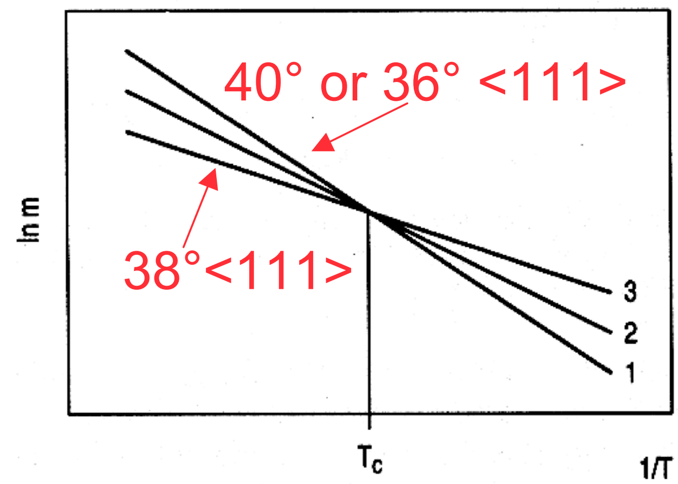

Gottstein, Shvindlerman et al.

This work: boundaries < 10° from 111

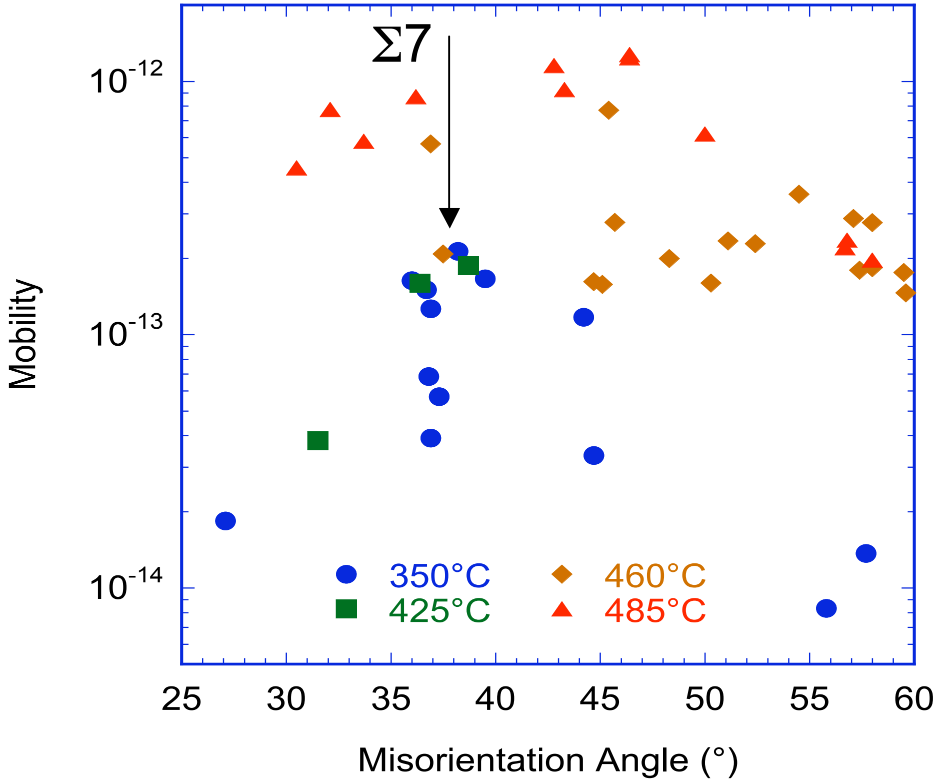

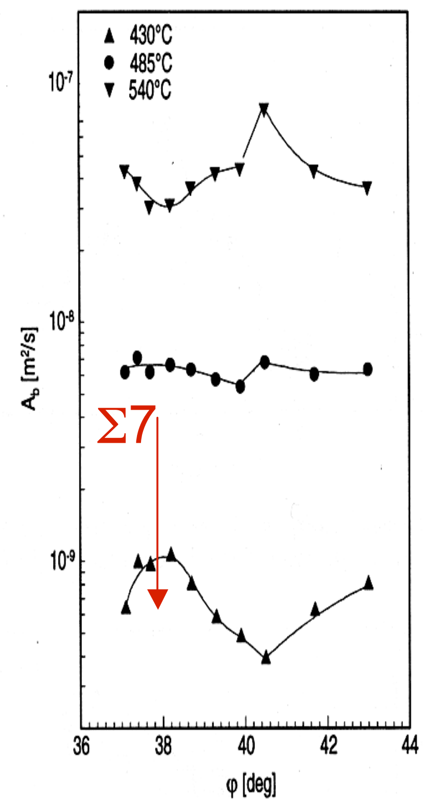

Mobility: Summary

- The classically observed maximum in mobility at 38°<111> is verified (Σ7).
- A compensation effect exists: low activation enthalpy for the Σ7 means that it exhibits a local minimum at high temperature and there is then a double peak, i.e. maximum at ~40°<111> (and at ~36°).
- The highly mobile Σ7 type exhibits strong inclination dependence (pure tilt is most mobile).
- Results are in agreement with experiments using curvature as a driving force (RWTH-Aachen). Also in agreement with MD simulations (Princeton, CSM).

Summary

- For all materials examined to date, and for almost all boundary types, the grain boundary energy is proportional to the average of the surface energies.
- The much used CSL theory for grain boundary energy, i.e. low sigma values predict low energies, is a poor predictor of the anisotropy. It does, however, play a minor role (local minima).
- For sufficiently random textures, grain growth leads to a steady-state g.b. population that is inverse to the energy anisotropy.
- Mobility is highly anisotropic in both experiment and simulation. The anisotropy is insensitive to the nature of the driving force. Peaks at "38°<111>" and "40°<111>" both exist - but, in different temperature and composition regimes.
- For *fcc* metals, plane edge matching (of close packed planes) correlates well with experimental and simulation results for mobility.
- Mobility anisotropy also strongly affects microstructural evolution in strongly textured materials: large changes in texture (and MDF) can occur.